

**Satellite Application Facility on Climate Monitoring**

**Scientific Report**

**Initial Validation of CM-SAF Cloud Products  
using MSG/SEVIRI Data**

**Reference Number:**

**SAF/CM/DWD/SMHI/KNMI/SR/CLOUDS/1**

**Issue/Revision Index:**

**1.0**

**Date:**

**23 March 2005**

	<b>Scientific Report</b> <b>Initial Validation of CM-SAF</b> <b>Cloud Products using</b> <b>MSG/SEVIRI Data</b>	Doc. No: <b>SAF/CM/DWD/SMHI/KNMI/SR/CLOUDS/1</b> Issue: <span style="float: right;"><b>1.0</b></span> Date: <span style="float: right;"><b>23 March 2005</b></span>
---	--	--

**Document Signature Table**

	<b>Name</b>	<b>Function</b>	<b>Signature</b>	<b>Date</b>
<b>Author</b>	Karl-Göran Karlsson Erwin Wolters Peter Albert Anke Tetzlaff Rob Roebeling Werner Thomas Sheldon Johnston	Project scientists		
<b>Approval</b>	Annegret Gratzki	Science co-ordinator		
<b>Approval</b>				
<b>Release</b>	Martin Werscheck	Project manager		
<b>Eumetsat Approval</b>				

	<b>Scientific Report</b> <b>Initial Validation of CM-SAF</b> <b>Cloud Products using</b> <b>MSG/SEVIRI Data</b>	Doc. No: <b>SAF/CM/DWD/SMHI/KNMI/SR/CLOUDS/1</b> Issue: <span style="float: right;"><b>1.0</b></span> Date: <span style="float: right;"><b>23 March 2005</b></span>
---	--	--

### Document Change Record

Issue/Revision	Date	DCN No.	Changed Pages/Paragraphs
1.0	23.03.2005	SAF/CM/DWD/SMHI/KNMI/SR /CLOUDS/1	First Version

	<b>Scientific Report</b> <b>Initial Validation of CM-SAF</b> <b>Cloud Products using</b> <b>MSG/SEVIRI Data</b>	Doc. No: <b>SAF/CM/DWD/SMHI/KNMI/SR/CLOUDS/1</b> Issue: <span style="float: right;"><b>1.0</b></span> Date: <span style="float: right;"><b>23 March 2005</b></span>
---	--	--

**Distribution List**

Internal Distribution	
Name	No. Copies
DWD archive	1

External Distribution		
Company	Name	No. Copies
EUMETSAT		1

	<b>Scientific Report</b> <b>Initial Validation of CM-SAF</b> <b>Cloud Products using</b> <b>MSG/SEVIRI Data</b>	Doc. No: <b>SAF/CM/DWD/SMHI/KNMI/SR/CLOUDS/1</b> Issue: <span style="float: right;"><b>1.0</b></span> Date: <span style="float: right;"><b>23 March 2005</b></span>
---	--	--

## Table of Contents

<b>1</b>	<b>INTRODUCTION</b> .....	<b>1</b>
<b>2</b>	<b>CLOUD OBSERVATION AT THE CABAUW, CHILBOLTON AND PALAISEU OBSERVATION SITES</b> .....	<b>2</b>
2.1	INDIVIDUAL CLOUD OBSERVATION INSTRUMENTS .....	2
2.1.1	<i>Lidar</i> .....	2
2.1.2	<i>Cloud radar</i> .....	2
2.1.3	<i>Microwave radiometer</i> .....	2
2.1.4	<i>Pyranometer</i> .....	3
2.2	MEASUREMENT CAMPAIGNS .....	3
2.2.1	<i>CloudNET</i> .....	3
2.2.2	<i>CESAR</i> .....	3
<b>3</b>	<b>VALIDATION OF THE FRACTIONAL CLOUD COVER PRODUCT (CFC)</b> .....	<b>4</b>
3.1	VALIDATION METHOD.....	4
3.2	VALIDATION RESULTS FOR INDIVIDUAL OBSERVATIONS .....	5
3.3	VALIDATION RESULTS FOR AVERAGED OBSERVATIONS .....	8
3.4	SUMMARY OF CFC VALIDATION RESULTS .....	9
<b>4</b>	<b>VALIDATION OF THE CLOUD TYPE PRODUCT (CTY)</b> .....	<b>10</b>
4.1	DETAILS OF THE VALIDATION METHOD.....	11
4.2	RESULTS .....	13
4.3	SUMMARY OF CTY VALIDATION RESULTS.....	14
<b>5</b>	<b>VALIDATION OF THE CLOUD TOP PRODUCT (CTH/CTP/CTT)</b> .....	<b>15</b>
5.1	VALIDATION METHODS.....	15
5.1.1	<i>Cloud radar CTH retrievals</i> .....	15
5.1.2	<i>MSG/SEVIRI and NOAA/AVHRR CTH retrievals</i> .....	16
5.2	RESULTS .....	17
5.2.1	<i>Comparison between MSG/SEVIRI and Cloud radar CTH values</i> .....	17
5.2.2	<i>Comparison between MSG/SEVIRI, cloud radar and NOAA/AVHRR CTHs</i> .....	20
5.3	ADDITIONAL RESULTS FROM OTHER VALIDATION PERIODS.....	21
5.4	SUMMARY OF CTH/CTP/CTT VALIDATION RESULTS.....	22
<b>6</b>	<b>VALIDATION OF THE THERMODYNAMIC CLOUD PHASE PRODUCT (CPH)</b> .....	<b>23</b>
6.1	VALIDATION METHOD.....	23
6.2	RESULTS .....	24
6.3	SUMMARY OF CPH VALIDATION RESULTS .....	27
<b>7</b>	<b>VALIDATION OF THE OPTICAL THICKNESS PRODUCT (COT)</b> .....	<b>27</b>
7.1	VALIDATION METHOD.....	28
7.2	RESULTS .....	28
7.3	SUMMARY OF COT VALIDATION RESULTS.....	31
<b>8</b>	<b>VALIDATION OF THE CLOUD WATER PATH PRODUCT (CWP)</b> .....	<b>32</b>
8.1	VALIDATION METHOD.....	32
8.2	RESULTS .....	32
8.3	SUMMARY OF CLWP VALIDATION RESULTS .....	35
<b>9</b>	<b>SUMMARY AND CONCLUSIONS</b> .....	<b>36</b>

	<p align="center"><b>Scientific Report Initial Validation of CM-SAF Cloud Products using MSG/SEVIRI Data</b></p>	<p>Doc. No: <b>SAF/CM/DWD/SMHI/KNMI/SR/CLOUDS/1</b></p> <p>Issue: <span style="float: right;"><b>1.0</b></span></p> <p>Date: <span style="float: right;"><b>23 March 2005</b></span></p>
---	--	--

**10 REFERENCES.....38**

	<b>Scientific Report</b> <b>Initial Validation of CM-SAF</b> <b>Cloud Products using</b> <b>MSG/SEVIRI Data</b>	Doc. No: <b>SAF/CM/DWD/SMHI/KNMI/SR/CLOUDS/1</b> Issue: <span style="float: right;"><b>1.0</b></span> Date: <span style="float: right;"><b>23 March 2005</b></span>
---	--	--

## List of Tables

<a href="#"><u>Table 1.1</u></a> <i>The CM-SAF cloud products based on MSG/SEVIRI data</i> .....	1
<a href="#"><u>Table 3.1</u></a> <i>Heidke skill scores for Synop and SEVIRI cloud fractions</i> .....	8
<a href="#"><u>Table 3.2</u></a> <i>Mean cloud fraction from Synop measurements. Values are in octas</i> .....	8
<a href="#"><u>Table 3.3</u></a> <i>Mean cloud fraction from MSG measurements. Values are in octas</i> .....	9
<a href="#"><u>Table 3.4</u></a> <i>Absolute (and relative) deviation between MSG and synop cloud fraction. Values are in octas for absolute deviations and in percent for relative deviations (in parenthesis)</i> .....	9
<a href="#"><u>Table 4.1</u></a> <i>Percentage of matching cloud radar derived and MSG-derived CTY categories for the two different vertical separation approaches</i> .....	13
<a href="#"><u>Table 4.2</u></a> <i>Linear correlation coefficient (<math>R^2</math>), offset (for regression curve) and RMS error for daily cloud radar/MSG CTY frequencies</i> .....	14
<a href="#"><u>Table 4.3</u></a> <i>Comparison of cloud radar retrieved monthly cloud frequencies and MSG retrieved monthly cloud frequencies</i> .....	14
<a href="#"><u>Table 5.1</u></a> <i>Linear correlation coefficient (<math>R^2</math>) and RMS error for the cloud radar and MSG/SEVIRI CTH comparison. Max/mean MSG/SEVIRI: Maximum and mean cloud top height derived from a 20 x 20 km MSG/SEVIRI box centred over the cloud radar site. Max/mean radar: Maximum and mean CTH detected by the radar device in a 30-minute time window centered at the satellite acquisition time</i> .....	19
<a href="#"><u>Table 5.2</u></a> <i>Linear correlation coefficient (<math>R^2</math>) and RMS error for the daily cloud radar and daily MSG/SEVIRI comparison</i> .....	20
<a href="#"><u>Table 5.3</u></a> <i>Linear correlation coefficient (<math>r^2</math>) and RMS error for the NOAA/AVHRR and MSG/SEVIRI comparison. The max/min NOAA/AVHRR and MSG/SEVIRI refers to the maximum and mean cloud top height derived from 9 x 9 km (NOAA/AVHRR) or 20 x 20 km boxes (MSG/SEVIRI) centred around the corresponding cloud radar</i> .....	21
<a href="#"><u>Table 6.1</u></a> <i>Contingency table of collocated cloud thermodynamic phase for Cabauw (a) and Chilbolton (b). Included are cases with satellite cloud cover &gt; 80% and optical thickness <math>\tau &gt; 0</math>. Cabauw: n=205, Chilbolton: n=217</i> .....	24
<a href="#"><u>Table 7.1</u></a> <i>Summary of comparison of MSG and pyranometer derived Cloud Optical Thickness</i> .....	31
<a href="#"><u>Table 8.1</u></a> <i>Summary of the comparison of MSG (Meteosat-8) and Microwave derived Cloud Liquid Water Path</i> .....	35
<a href="#"><u>Table 9.1</u></a> <i>Validation results for the CM-SAF cloud products for the SIVVRR V2 review. Results are given for evaluation of individual (instantaneous), daily and monthly estimations (where applicable)</i> .....	36

	<b>Scientific Report</b> <b>Initial Validation of CM-SAF</b> <b>Cloud Products using</b> <b>MSG/SEVIRI Data</b>	Doc. No: <b>SAF/CM/DWD/SMHI/KNMI/SR/CLOUDS/1</b> Issue: <span style="float: right;"><b>1.0</b></span> Date: <span style="float: right;"><b>23 March 2005</b></span>
---	--	--

## List of Figures

<a href="#"><u>Figure 3.1 Geographical location of Synop stations used for SEVIRI cloud mask validation</u></a> .....	4
<a href="#"><u>Figure 3.2 Frequencies of occurrence of synop observations for given MSG cloud fractions</u></a> .....	6
<a href="#"><u>Figure 3.3 Frequencies of occurrence of MSG observations for given synop cloud fractions</u></a> .....	7
<a href="#"><u>Figure 4.1 Daily cloud type frequencies retrieved (%) from cloud radar data plotted against daily cloud type frequencies (%) retrieved from MSG CTY estimations. <b>Left</b>) Chilbolton cloud radar, <b>right</b>) Cabau cloud radar</u></a> .....	13
<a href="#"><u>Figure 5.1 MSG/SEVIRI cloud top heights (CTH) plotted against radar-retrieved CTHs. <b>Left</b>) Chilbolton ground station. <b>Right</b>) Cabauw ground station. <b>Upper</b>) Maximum CTH value in a 20 x 20 km MSG/SEVIRI box plotted against maximum cloud radar CTH in a 30 minute time window; red = semi-transparent, green = opaque, black = less than 50 % cloud coverage. <b>Middle</b>) Mean MSG/SEVIRI CTH plotted against mean radar CTH; red = semi-transparent, green = opaque, black = less than 50 % cloud coverage. <b>Lower</b>) Mean MSG/SEVIRI CTH plotted against minimum and maximum radar CTH values within the 30 minute time window</u></a> .....	18
<a href="#"><u>Figure 5.2 Daily averaged MSG/SEVIRI cloud top heights (CTH) plotted against daily averaged radar retrieved CTHs. <b>Left</b>) Chilbolton ground station. <b>Right</b>) Cabauw ground station</u></a> .....	20
<a href="#"><u>Figure 5.3 <b>Left</b>: Scatterplot of all simultaneous CTT retrievals from MSG/SEVIRI and NOAA/AVHRR (PPS – although, here only showing results from NOAA-16) during the month of October 2004. <b>Right</b>: Corresponding CTT histogram for the two methods (MSG and PPS)</u></a> .....	22
<a href="#"><u>Figure 5.4 Results of the inter-comparison between simultaneous AVHRR and SEVIRI CTH retrievals using the highest layer approach (i.e., highest LIDAR layer is compared to the highest satellite layer) for the SIRTA LIDAR site in the period March-July 2004 (see Trolez et al., 2005)</u></a> .....	23
<a href="#"><u>Figure 6.1 Daily skill of the satellite water and ice phase retrieval for Cabauw (upper graph) and Chilbolton (lower graph). Cloud cover and optical thickness thresholds as in Table 6.1</u></a> .....	25
<a href="#"><u>Figure 6.2 Cloud radar at Cabauw, May 2<sup>nd</sup> 2004, 8:00-16:30 UTC. Cloud thermodynamic phase retrievals are superposed for MSG (upper bars) and the lidar/radar algorithm (lower bars), with a red bar representing water and a blue bar representing ice</u></a> .....	26
<a href="#"><u>Figure 6.3 Cloud radar at Cabauw, May 9<sup>th</sup> 2004, 8:00-16:30 UTC. Cloud thermodynamic phase retrievals are superposed for MSG (upper bars) and the lidar/radar algorithm (lower bars), with a red bar representing water and a blue bar representing ice</u></a> .....	27
<a href="#"><u>Figure 7.1 Frequency distributions of MSG-1 (Meteosat-8) and pyranometer -derived cloud optical thickness for Cabauw, The Netherlands. The upper two distributions were made for April 14<sup>th</sup> till April 30<sup>th</sup> 2004, the lower two distributions for May 2004</u></a> .....	29
<a href="#"><u>Figure 7.2 Frequency distributions of differences between pyranometer and MSG-1 (METEOSAT-8) derived cloud optical thickness for April 14<sup>th</sup> till April 30<sup>th</sup> 2004 (left panel) and May 2004 (right panel) for Cabauw, The Netherlands</u></a> .....	30
<a href="#"><u>Figure 7.3 Scatter plots of pyranometer and MSG-derived COT for Cabauw, The Netherlands. Left panel: April 14<sup>th</sup> till April 30<sup>th</sup> 2004, right panel: May 1<sup>st</sup> till May 31<sup>st</sup> 2004</u></a> .....	31
<a href="#"><u>Figure 8.1 Example of time series (left) and scatter plot (right) of MSG and microwave radiometer liquid water path for May 1<sup>st</sup> 2004 for Chilbolton, UK</u></a> .....	33

	<b>Scientific Report</b> <b>Initial Validation of CM-SAF</b> <b>Cloud Products using</b> <b>MSG/SEVIRI Data</b>	Doc. No: <b>SAF/CM/DWD/SMHI/KNMI/SR/CLOUDS/1</b> Issue: <span style="float: right;"><b>1.0</b></span> Date: <span style="float: right;"><b>23 March 2005</b></span>
---	--	--

*Figure 8.2* *Frequency distributions of MSG (METEOSAT-8) and microwave radiometer derived cloud liquid water path for Chilbolton, UK. The upper two distributions were made for the period of April 14<sup>th</sup> till April 30<sup>th</sup> 2004 and the lower two distributions for the period of May 2004.....* 34

*Figure 8.3* *Frequency distributions of differences between microwave and MSG (METEOSAT-8) derived cloud liquid water path for April 14<sup>th</sup> till April 30<sup>th</sup> (left panel) and May 2004 (right panel) for Chilbolton, UK.*35

## 1 INTRODUCTION

This report presents the results of a first validation of the MSG/SEVIRI cloud products for the CM-SAF. It was prepared for the System Integration Validation and Verification Readiness Review for the second version of the CM-SAF production system (CM-SAF SIVVRR V2).

The CM-SAF cloud products and their main characteristics (i.e., notation, spatial and temporal resolution) are summarised in the following Table 1.1:

**Table 1.1** *The CM-SAF cloud products based on MSG/SEVIRI data*

Product	Acronym	Resolution			
		Spatial	Temporal		
			Daily	Monthly	MMDC (Monthly Mean Diurnal Cycle)
Fractional cloud cover	CFC	15 km	✓	✓	✓
Cloud type	CTY	15 km	✓	✓	✓
Cloud top temperature, height, and pressure	CTT, CTH, CTP	15 km	✓	✓	✓
Cloud phase	CPH	15 km	✓	✓	✓
Cloud optical thickness	COT	15 km	✓	✓	✓
Cloud water path	CWP	15 km	✓	✓	✓

All products will be shortly introduced and described below in association with the presentation of validation results. However, for a detailed description of product content and methodology the reader is referred to the CM-SAF User Manual of Products (CM-SAF UMP, 2005).

The goal for the validation activity has been to provide results from a comprehensive validation exercise based on at least one full month of data for which all cloud products have been validated simultaneously. Due to the need to have validating observations available simultaneously for all products, the chosen period was the period between 15<sup>th</sup> of April to 14<sup>th</sup> of May 2004. The most important limiting factor for this particular choice of period was the need to have simultaneous measurements from cloud radars, microwave radiometers and other instruments to enable a proper validation of all cloud products. The chosen period could offer the most extensive validation data set, thus fulfilling the needs for this particular validation activity. However, for some of the products (e.g., the fractional cloud cover product and the cloud top products) also other periods are covered. This would give at least a preliminary indication on whether the results are valid also for other seasons. A more definite answer to this question will be provided later in connection to the next review (Operational Readiness Review – ORR V2) where a more extensive validation data set will be presented for all products. Finally, it should be mentioned that some references and comparisons are also made to the corresponding NOAA AVHRR products (which were subject to validation activities in the previous CM-SAF ORR V1 review).

In the following, sections 3 to section 8 describe the used observations, the validation methods and the detailed validation results for each of the validated six cloud products. Finally, section 9

	<b>Scientific Report</b> <b>Initial Validation of CM-SAF</b> <b>Cloud Products using</b> <b>MSG/SEVIRI Data</b>	Doc. No: <b>SAF/CM/DWD/SMHI/KNMI/SR/CLOUDS/1</b> Issue: <span style="float: right;"><b>1.0</b></span> Date: <span style="float: right;"><b>23 March 2005</b></span>
---	--	--

gives a short summary of all validation results and a discussion on the product maturity and any possible consequences concerning future development efforts. Since the validation data sets from a few particularly chosen observation sites are fundamental for the validation of many of the products, these are first described in the section 2 prior to the presentation of the results.

## **2 CLOUD OBSERVATION AT THE CABAUW, CHILBOLTON AND PALAISEU OBSERVATION SITES**

### **2.1 Individual cloud observation instruments**

In this sub-section a summary is given of the instruments that were used to measure cloud physical parameters and which have been used in this study to validate a majority of the CM-SAF cloud products.

#### **2.1.1 Lidar**

The lidar is a high power laser that emits short pulses of light. The light scattered back from atmospheric particles and molecules is recorded in a time-gated fashion. The time of flight between emission of the laser pulse and reception of the echo is used to measure the range at which the backscattering has occurred.

Depending on wavelength, lidar is most sensitive to particles with radii between 1 and 3  $\mu\text{m}$ , which are typically radii of cloud water particles.

#### **2.1.2 Cloud radar**

The cloud radar measures two cloud physical parameters, namely the distance between the instrument and the cloud particles and the velocity of the moving particles. The cloud radar is most sensitive to scattering of particles with high effective radii but the maximum sensitivity in this respect depends also on the operating frequency. The two radars used here (in Cabauw and Chilbolton) operate at a frequency of 35 GHz leading to an operational wavelength of 8.6 mm which makes it sensible to cloud droplets within the range of 0 to about 200 micron (Rayleigh scattering regime). Considering these radii it is not surprising that the cloud radar is especially suited to measure the particle volume and moving velocity of ice crystals (Donovan *et al.*, 1998).

The finite travel time of the signal from the radar to a target and back causes a frequency difference between the transmitted and received signal. This frequency difference can be obtained by multiplying the transmitted signal and the received signal (mixing) and combine this with low pass filtering of the mixed signal. The resulting signal is called the beat signal. The frequency of the beat signal is directly related to the distance of the target. Further, cloud radar measures the Doppler shift of moving particles. By measuring this shift, the velocity of the targets can be determined. The frequencies in the beat signal are, however, already used to determine the distance of the target. The velocities can still be obtained by measuring the phase shifts for succeeding sweeps.

#### **2.1.3 Microwave radiometer**

Microwave radiometers measure incoherent radiant electromagnetic energy. From the ground, zenith-pointing radiometers measure energy radiated (emitted) by atmospheric gases and liquid water in the form of cloud droplets and rain. This energy is dependent on the measurement frequency and is proportional to the amount of material present in the atmosphere. Radiometer

	<b>Scientific Report</b> <b>Initial Validation of CM-SAF</b> <b>Cloud Products using</b> <b>MSG/SEVIRI Data</b>	Doc. No: <b>SAF/CM/DWD/SMHI/KNMI/SR/CLOUDS/1</b> Issue: <span style="float: right;"><b>1.0</b></span> Date: <span style="float: right;"><b>23 March 2005</b></span>
---	--	--

measurements at selected frequencies are used to make estimates of integrated water vapor path (WVP) and liquid water path (LWP).

The technique to relate sky brightness temperature (BT) at two or more frequencies to WVP and LWP is accomplished by constructing Look Up Tables (described as a Training Set) of WVP, LWP, and corresponding BT<sub>i</sub> values. Measurements of BT<sub>i</sub> from the radiometers can then be transformed into estimates of WVP and LWP.

#### **2.1.4 Pyranometer**

The thermoelectric pyranometer is an instrument that can accurately measure broadband hemispherical irradiance in the solar spectral region. Pyranometers are mainly used at meteorological stations to measure the downwelling solar irradiance at the surface. It can either measure the global or the diffuse irradiance. The accuracy of standard pyranometers should be about 3% according WMO standards. However, mean solar irradiances may be underestimated by 3 – 8% due to pollution on the instrument dome, thermal cooling of the detectors and long maintenance intervals (Deneke, 2002).

### **2.2 Measurement campaigns**

In this sub-section a summary is given of the measurement campaigns that were used to acquire the cloud observations for the validation of MSG/SEVIRI-derived cloud physical parameters in the CM-SAF project.

#### **2.2.1 CloudNET**

CloudNET is a EU-funded research project that aims to use data obtained quasi-continuously at three remote sensing stations for the development and implementation of cloud remote sensing synergy algorithms. The project started on 1st of April 2001 and will end on 1st April 2005. The three experimental research sites are situated in Cabauw (The Netherlands), Chilbolton (UK) and Palaiseau (France). Each site is equipped with radar, lidar and a suite of passive instrumentation. The use of active instruments (lidar and cloud radar) results in detailed vertical profiles of important cloud parameters, which cannot be derived from current satellite sensing techniques. For these already existing cloud remote sensing stations (CRS-stations) a network will be operated for at least a two year period (2003-2004) to build a co-coordinated, harmonized and joint data archive. The observations will be used to evaluate four operational numerical models and to demonstrate the role that could be played by an operational network of cloud remote sensing stations.

#### **2.2.2 CESAR**

The Cabauw Experimental Site for Atmospheric Research (CESAR) is located in The Netherlands. The site consists of a large set of instruments to study the atmosphere and its interaction with the land surface. The CESAR objectives are monitoring of long-term tendencies in atmospheric changes, studies of atmospheric and land surface processes for climate modeling, validation of space-borne observations and development and implementation of new measurement techniques. Monitoring operations started in 2000 and will continue till 2010 or later. The site is equipped with remote sensing instruments, in situ tower instruments and in situ ground instruments. Among others, instruments like lidar, radar, ceilometer and pyranometer are operated.

	<b>Scientific Report</b> <b>Initial Validation of CM-SAF</b> <b>Cloud Products using</b> <b>MSG/SEVIRI Data</b>	Doc. No: <b>SAF/CM/DWD/SMHI/KNMI/SR/CLOUDS/1</b> Issue: <span style="float: right;"><b>1.0</b></span> Date: <span style="float: right;"><b>23 March 2005</b></span>
---	--	--

### 3 VALIDATION OF THE FRACTIONAL CLOUD COVER PRODUCT (CFC)

In the framework of the CM-SAF, the MSG/SEVIRI cloud mask developed by the Nowcasting SAF is routinely applied to SEVIRI measurements. The cloud masking algorithm applied to MSG SEVIRI data is a multi-spectral thresholding algorithm making use of dynamically adjusted thresholds. These are pre-calculated using radiative transfer calculations where input data sets such as physiography (e.g. land use, topography, etc.) and Numerical Weather Prediction (NWP) analyses are used. The methodology is described more in detail by Derrien and LeGleau (2003) and in SAFNWC SUM/1 (2004).

For validation of both instantaneous and averaged products, three months of MSG/SEVIRI data have been compared to Synop observations (April, May and October 2004). Figure 3.1 shows the geographical location of all used Synop stations, subdivided into land stations, ship and buoy measurements. Stations identified as ship measurements but clearly located on land are mobile stations. The stations are further divided in two regions, one covering central Europe and the eastern Atlantic, the other covering the central Atlantic. This artificial subdivision is only due to limited processing time and will be extended in further studies.

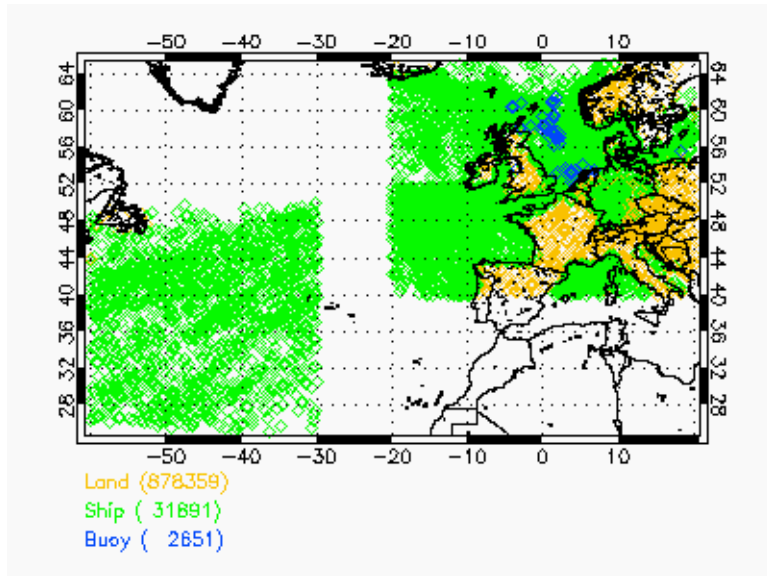


**Figure 3.1** Geographical location of Synop stations used for SEVIRI cloud mask validation

#### 3.1 Validation method

When Synop observations are compared to satellite measurements the strongly differing viewing techniques have to be properly considered. While the satellite instrument is downward looking with, in the case of SEVIRI, a pixel size between 3 and 15 km depending on geographic latitude, the ground-based observer is upward-looking, reporting one observation representative for more or less the complete visible sky. Additionally, different quantities are reported: While the SEVIRI observation is divided in 4 classes (clear sky, cloudy, fractional clouds, snow or ice on the ground) the synop observation provides a cloud fraction in octa. Here, 0 octa stands for no cloud visible at all, while 8 octa stands for completely overcast sky. As soon as one cloud is visible, 1 octa are reported while as soon as one hole in the cloud cover is visible, 7 octa are reported.

	<b>Scientific Report</b> <b>Initial Validation of CM-SAF</b> <b>Cloud Products using</b> <b>MSG/SEVIRI Data</b>	Doc. No: <b>SAF/CM/DWD/SMHI/KNMI/SR/CLOUDS/1</b> Issue: <span style="float: right;"><b>1.0</b></span> Date: <span style="float: right;"><b>23 March 2005</b></span>
---	--	--

Between 2 and 6 octa, the observation should represent the actual cloud fraction above the synop station.

Additionally, the different temporal sampling of the measurements has to be considered. Synop observations are either made hourly or in 3 or 6 hours intervals, respectively. MSG-1 measurements are available with a 15 minutes time interval. As all synop measurements are done at the full hour, the MSG-1 slot starting 15 minutes before was chosen for comparison. Scanning starts at the South Pole thus effectively reducing the time difference to less than 10 minutes.

The following approach was chosen for the comparison of SEVIRI and Synop observations: For all Synop observations, all SEVIRI pixels from the closest time slot within a radius of 30 km around the synop station were considered. In a first step, the quality flag provided by the MSG processing software was analysed in order to exclude pixels analysed with a low confidence from further processing. In a second step, the cloud fraction above the Synop stations was calculated from the remaining MSG pixels:

$$CFC_{MSG} = \frac{\sum \text{cloudy} + 0.5 \sum \text{fractional clouds}}{\sum \text{all pixels}}$$

The numerator is calculated from the sum of all pixels classified either as cloudy or partly cloudy, the latter multiplied by 0.5 in order to correct for the fact that fractional clouds do not completely fill the satellite's field of view. The denominator is calculated from the sum of all valid pixels, i.e. pixels which have not been classified as undecided and who don't show the low confidence flag.

Then the cloud fraction was converted to octa in order to allow an easy comparison with the synop observations. Additionally, in order to mimic the special treatment of octa levels 0 and 8 in the synop observations, only MSG cloud fractions less than 0.01 were kept in the "1 octa" class and only MSG cloud fractions greater than 0.99 were kept in the "8 octa" class.

### 3.2 Validation results for individual observations

In the first step, the individual Synop observations were compared to their MSG counterparts.

Figure 3.2 shows the frequencies of occurrence of the different Synop observations for any given MSG cloud fraction between 0 and 9. These numbers represent how strongly a given MSG observations is confirmed by the Synop data. The figure combines all comparisons over land from all three months. The best agreement between MSG and Synop can be seen for the full overcast classes of 7/8 and 8/8. Here, only a relatively small number of synop observations differ significantly from the MSG results. The situation is slightly worse for the clear sky cases. When MSG "reports" 0/8 almost 45 % of synop observations fall in the classes 1/8 and higher. The intermediate classes show a somewhat indifferent behaviour, with almost all synop classes occurring significantly often for a given MSG class.

Now the opposite question also has to be considered: How good do the MSG results represent the Synop observations? Figure 3.3 therefore shows very similar histograms, now showing the frequency of occurrence of MSG observations for any given Synop cloud fraction.



**Scientific Report  
Initial Validation of CM-SAF  
Cloud Products using  
MSG/SEVIRI Data**

Doc. No: **SAF/CM/DWD/SMHI/KNMI/SR/CLOUDS/1**  
Issue: **1.0**  
Date: **23 March 2005**

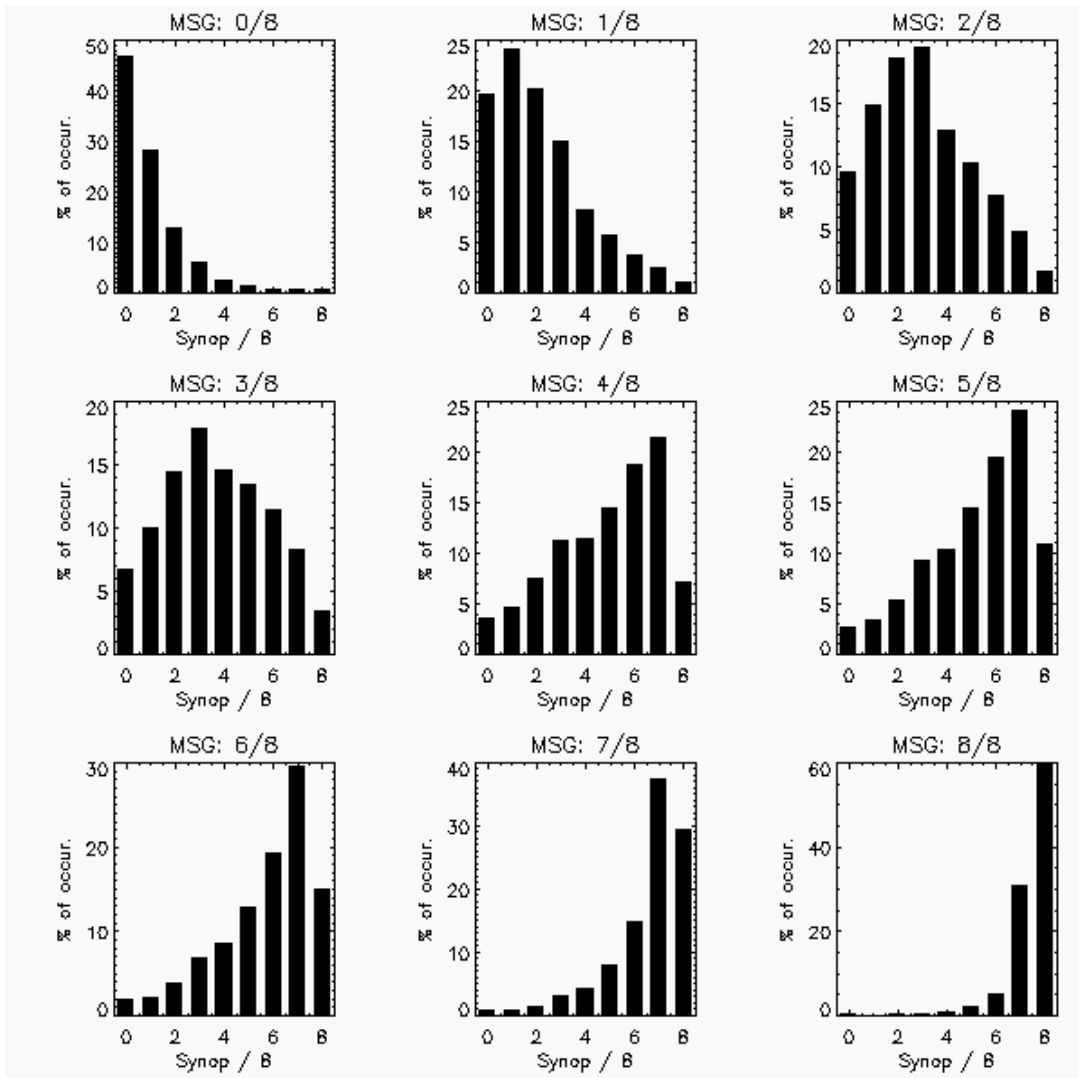


**Figure 3.2** Frequencies of occurrence of synop observations for given MSG cloud fractions.

Here the situation is somewhat improved, at least with regard to the “clear sky” and “fully overcast” classes. For the intermediate classes between 2 and 6 octas it has to be noted that no correction whatsoever was performed in order to correct for the slanted view of the ground based observer with increasing viewing zenith. All MSG pixels were equally weighted not taking into account the distance to the Synop station. Additionally, the parallax effect of the MSG observations, leading to the fact that high clouds are falsely displayed north of their true position in SEVIRI scenes, has not been corrected for here.

It is a bit tedious to discuss histograms like this for all months individually and for all types of Synop observations (land, ship, buoy). We therefore calculated the Heidke skill score for all different cases in order to provide simple scalar values which describe the overall performance of the cloud mask. The Heidke skill score can be calculated for any accordance matrix A, in our case a 9x9 matrix, as follows:



**Scientific Report  
Initial Validation of CM-SAF  
Cloud Products using  
MSG/SEVIRI Data**

Doc. No: **SAF/CM/DWD/SMHI/KNMI/SR/CLOUDS/1**  
Issue: **1.0**  
Date: **23 March 2005**

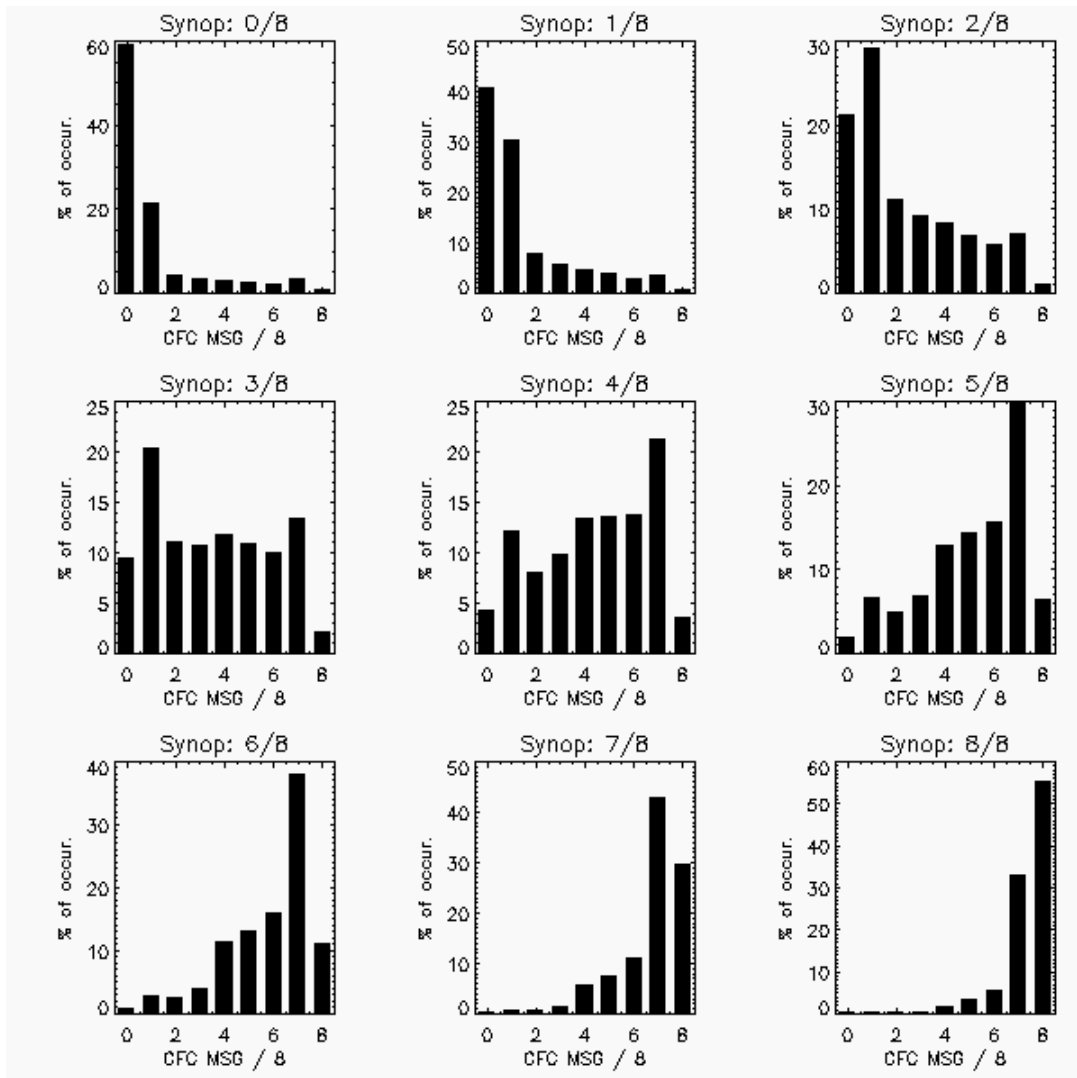


**Figure 3.3** Frequencies of occurrence of MSG observations for given synop cloud fractions.

$$HSS = \frac{N \sum_i A_{i,i} - \sum_i \left( \sum_j A_{i,j} \cdot \sum_j A_{j,i} \right)}{N^2 - \sum_i \left( \sum_j A_{i,j} \cdot \sum_j A_{j,i} \right)}$$

Here, N denotes the sum over all entries in the Matrix A, i.e. the total number of collocations. The Heidke skill score is 1 if the accordance matrix is diagonal, i.e. if the observations perfectly matched the assumed truth. It is -1 if the accordance matrix is anti diagonal and 0 if the accordance matrix is random.

	<b>Scientific Report</b> <b>Initial Validation of CM-SAF</b> <b>Cloud Products using</b> <b>MSG/SEVIRI Data</b>	Doc. No: <b>SAF/CM/DWD/SMHI/KNMI/SR/CLOUDS/1</b>
		Issue: <span style="float: right;"><b>1.0</b></span>
		Date: <span style="float: right;"><b>23 March 2005</b></span>

The Heidke skill score as a function of month and Synop observation type is shown in Table 3.1. It can be seen that the performance of the MSG cloud mask measured on individual Synop observations is relatively poor with skill scores of 0.26 at maximum. This reflects the comment already made with regard to the histograms in the previous figures. They show that the off-diagonal elements of the accordance matrix are not negligible.

**Table 3.1** *Heidke skill scores for Synop and SEVIRI cloud fractions*

	April 2004	May 2004	October 2004	<b>All</b>
Land	0.26	0.25	0.19	0.23
Ship	0.20	0.22	0.14	0.17
Buoy	0.14	0.10	0.12	0.12
All	0.26	0.25	0.19	0.23

### 3.3 Validation results for averaged observations

For the CM-SAF, especially the performance of the derived products with respect to averaged results is important. We therefore calculated monthly mean values of cloud fraction from Synop observations and MSG results, respectively. The results are shown in Tables 3.2-3.5. They show the averaged cloud fraction from Synop observations and from MSG measurements and the absolute and relative deviations. The agreement for land stations is significantly better than for ship and buoy observations, except for October, where the agreement between ship observations and MSG is better and the MSG cloud fraction is significantly smaller than the Synop cloud fraction. Overall, the bias of the MSG cloud fraction with respect to Synop observations is around -1 % for land, 5 % for ships and 11 % for buoys. The total bias is dominated by the land data due to their much larger number and is ~ -1 %.

The spatial distribution of deviations was also calculated by averaging all derived and observed cloud fractions on a 2°x2° grid. The relatively large grid size was necessary in order to get a significant number of ship observations within one grid. The minimum number of observations was 10, which of course is not enough to actually represent a proper monthly mean; however, the dataset can well be used for the comparison of averaged MSG and synop results. Figure 3.4 shows the results. It reflects the findings from the previous table, with very good agreement over land and a general overestimation of cloud fraction by MSG over sea.

**Table 3.2** *Mean cloud fraction from Synop measurements. Values are in octas.*

	April 2004	May 2004	October 2004	<b>All</b>
Land	5.04	5.48	5.54	5.32
Ship	5.17	5.47	5.61	5.46
Buoy	5.69	5.67	6.00	5.79
All	5.04	5.48	5.55	5.33

	<b>Scientific Report</b> <b>Initial Validation of CM-SAF</b> <b>Cloud Products using</b> <b>MSG/SEVIRI Data</b>	Doc. No: <b>SAF/CM/DWD/SMHI/KNMI/SR/CLOUDS/1</b> Issue: <span style="float: right;"><b>1.0</b></span> Date: <span style="float: right;"><b>23 March 2005</b></span>
---	--	--

**Table 3.3** Mean cloud fraction from MSG measurements. Values are in octas.

	April 2004	May 2004	October 2004	<b>All</b>
Land	5.08	5.53	5.31	5.26
Ship	5.63	5.94	5.68	5.73
Buoy	6.22	6.53	6.64	6.45
All	5.09	5.55	5.33	5.28

**Table 3.4** Absolute (and relative) deviation between MSG and synop cloud fraction. Values are in octas for absolute deviations and in percent for relative deviations (in parenthesis)

	April 2004	May 2004	October 2004	<b>All</b>
Land	0.04 (0.7)	0.05 (1)	-0.24 (-4.2)	-0.06 (-1.1)
Ship	0.46 (8.9)	0.47 (8.5)	0.07 (1.2)	0.27 (4.9)
Buoy	0.53 (9.4)	0.86 (15.1)	0.65 (10.8)	0.65 (11.3)
All	0.05 (1.0)	0.07 (1.3)	-0.22 (-3.9)	-0.04 (-0.8)

### 3.4 Summary of CFC validation results

An initial validation of the NWCSAF MSG SEVIRI cloud mask algorithm was performed with Synop observations. Synop observations of cloud fractions were compared to cloud fractions calculated from MSG observations within 30 km of the Synop stations. The individual comparisons show a relatively good agreement in the extreme cases clear sky and fully overcast. However, a significant number of observations disagree strongly when either Synop or MSG report medium cloud fractions. It has to be further investigated whether this is really due to algorithm shortcomings or due to the simple approach when comparing Synop and satellite measurements not taking into account the specific viewing geometry.

Averaged values agree much better, however, showing an overall underestimation of cloud fraction by MSG of approximately 1 %. Although, it has to be noticed that deviations are larger in the month of October (-3.9 %) which possibly indicates a seasonal variation in quality. This must be investigated further in the validation activities for the next ORR V2 review.

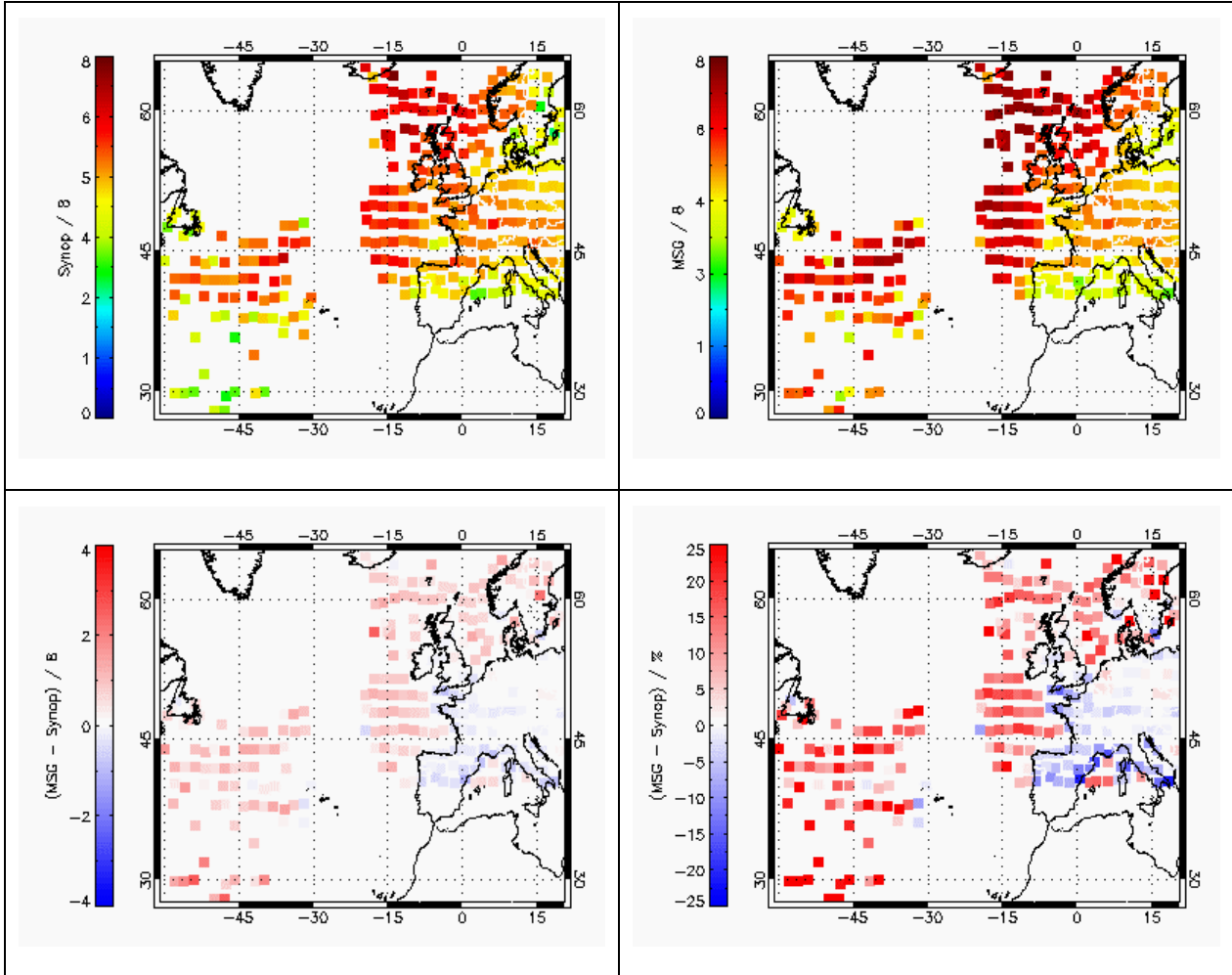


**Figure 3.4** Mean cloud fraction from synop observations (upper left) and from MSG measurements (upper right). Absolute (lower left) and relative deviations (lower right)

#### 4 VALIDATION OF THE CLOUD TYPE PRODUCT (CTY)

One of the operational cloud products provided by the CM-SAF are daily and monthly averages of cloud type frequencies derived from MSG/SEVIRI data. The MSG cloud type product (CTY) is generated using a multispectral thresholding algorithm and the detailed methodology is described by Derrien and LeGleau (2003) and in SAFNWC SUM/1 (2004). The cloud type assignments of the NWC-SAF product are grouped by the CM-SAF into **five** categories (**Low level clouds**, **Mid level clouds**, **High opaque clouds**, **High semi-transparent clouds** and **Fractional clouds**) and for each of this categories daily and monthly cloud frequencies are computed (further detailed in CM-SAF UMP, 2005).

The validation of cloud type categorisations is not a straight-forward and obvious procedure if being based on ordinary Synop observations (as a contrast to the previous case of validating the CFC product). The reason is that the different geometrical observation conditions (i.e., satellite

	<b>Scientific Report</b> <b>Initial Validation of CM-SAF</b> <b>Cloud Products using</b> <b>MSG/SEVIRI Data</b>	Doc. No: <b>SAF/CM/DWD/SMHI/KNMI/SR/CLOUDS/1</b> Issue: <span style="float: right;"><b>1.0</b></span> Date: <span style="float: right;"><b>23 March 2005</b></span>
---	--	--

viewing downward from top of atmosphere while the surface observer is viewing upward from the surface) make comparisons very difficult. For example, in cases of multi-layered cloudiness the surface may report exclusively low-level clouds while the satellite reports exclusively mid-level or high-level clouds. In this case it is impossible to evaluate the skill of the observation/interpretation since both the surface observation and the satellite interpretation fail in giving a correct description of true cloud conditions.

In this study we have chosen to carry out a limited validation exercise evaluating the CM-SAF MSG CTY frequencies by means of information provided by ground-based cloud radar data. The motivation is that we believe that it is necessary to use observations capable of describing in a realistic way both the occurrence and the exact vertical location of cloud layers. Currently, this can only be offered by cloud radar measurements (although to some extent being limited by some detection problems for optically thin and high clouds). Furthermore, we have used the cloud radar data in combination with radiosonde measurements to assign cloud types to the cloud radar detected uppermost cloud layers (trying to simulate the satellite viewing conditions). These radar CTY assignments are here directly compared to the condensed cloud type categories of the MSG product. In addition, daily and monthly radar retrieved cloud category frequencies are computed and compared to the corresponding CM-SAF MSG cloud category frequencies.

#### 4.1 Details of the validation method

Cloud height data, retrieved from radar profiles of the two cloud radar ground stations in Chilbolton and Cabauw, were compared to radiosonde measurements of De Bilt (The Netherlands; 52.10 N, 5.18 E) and corresponding cloud pressure and cloud temperature data were retrieved. It is important to note here that the location of the radiosonde measurements does not correspond exactly to the location of the two cloud radar stations (especially not in the case of the Chilbolton site). Consequently, the pressure and temperature assignments have thus to be regarded as rather rough estimates in the Chilbolton case. The cloud radar data used for this validation study covers the period April 15<sup>th</sup> to May 14<sup>th</sup> 2004. Similar to the cloud top height validation study (see next section), a 30 min averaged CTH value was available nearly continuously from 8 am to 5 pm for the study period.

A crucial question for the cloud type validation task is to find a commonly agreed definition of how to define the main cloud groups Low-level, Mid-level and High-Level clouds. Normally this definition is surface observation oriented, i.e., based on cloud-base altitudes rather than on cloud-top altitudes. The current two CM-SAF CTY algorithms (one for NOAA AVHRR and one for MSG/SEVIRI) are unfortunately using slightly different definitions or interpretations for this separation. Because of this circumstance we find it necessary to examine both approaches to see whether this difference in definition will be significant or not for the results.

The first approach (here denoted **Plain pressure level approach**) corresponds to the implementation in the CM-SAF NOAA AVHRR CTY method (further detailed in Dybbroe et al, 2005 and in SAFNWC SUM/2, 2004). CTY values are here assigned using infrared brightness temperature thresholds  $T$  defined according to the temperature (K) of the corresponding pressure levels (in hPa):

- Low level cloud:  $T > T_{800hPa}$
- Mid level cloud:  $T_{500hPa} < T < T_{800hPa}$
- High level cloud:  $T < T_{500hPa}$

	<b>Scientific Report</b> <b>Initial Validation of CM-SAF</b> <b>Cloud Products using</b> <b>MSG/SEVIRI Data</b>	Doc. No: <b>SAF/CM/DWD/SMHI/KNMI/SR/CLOUDS/1</b> Issue: <span style="float: right;"><b>1.0</b></span> Date: <span style="float: right;"><b>23 March 2005</b></span>
---	--	--

The second approach (denoted **Complex pressure level approach**), which is valid for the MSG/SEVIRI CTY algorithm, classifies clouds using the following temperature thresholds  $T$  (K):

- Low level cloud:  $T > 0.8 * T_{850hPa} + 0.2 * T_{700hPa} - 8$
- Mid level cloud:  $0.8 * T_{850hPa} + 0.2 * T_{700hPa} - 8 > T > 0.5 * T_{500hPa} - 0.2 * T_{700hPa} + 178$
- High level cloud:  $T < 0.5 * T_{500hPa} - 0.2 * T_{700hPa} + 178$

If comparing the two approaches it is clear that there are similarities but also differences. It should be mentioned that the **Complex pressure level approach** resulted from extensive training target studies. Analysts with long experience from synoptical weather forecasting participated and for them the **Plain pressure level approach** was considered inadequate to match the subjective interpretation of cloud types used in weather forecasting applications.

One CTY assignment was provided for each 30-minute radar time window according to the corresponding averaged cloud top radar height. Daily radar cloud category frequencies were computed by calculating the percentage of low-, mid- and high-level clouds from 30 min cloud type assignments for each measurement day. Single cloud radar samples in high temporal resolution (intervals of a few seconds) were not available for this validation study. Consequently, only a maximum number of 20 CTY assignments per day could be used to compute the daily radar cloud type statistics. Finally, daily radar cloud type frequencies were added and averaged to compute a corresponding 30-day average for the Cabauw and Chilbolton sites.

MSG CTY frequencies were calculated approximately similar to the CM-SAF averaging algorithms. In a 20 km x 20 km pixel window centered around the cloud radar stations, MSG/SEVIRI CTY values were retrieved and re-classified into the categories 'Low-level clouds', 'Mid-level clouds' and 'High-level clouds'. Due to the fact that the cloud radar does not allow the discrimination between semi-transparent and opaque clouds, these two cloud groups were merged into one high-level cloud category. Furthermore, the category Fractional clouds is not studied at all here due to problems of making a proper definition of this cloud category in the cloud radar data set.

For the entire pixel window the percentage of each cloud type category was computed. Due to the risk of finding significant geometric MSG dislocations for high cloud layers (the parallax effect) at the latitude of the two ground radar stations, a pixel window instead of single MSG pixels was chosen for the inter-comparison. Daily averages were computed based on computed cloud type frequencies from hourly MSG data. The averaging was performed only for the time period 7:45 am to 16:45 pm MSG scenes to be coherent with the radar measurement period. For the direct cloud radar/satellite scene inter-comparisons, only MSG data assigned as being of good quality according to quality flag were used. A corresponding filtering of cloud radar data was made. The allowed cloud top height variability within the cloud radar time window was restricted to be less than 1000 m). However, daily and monthly statistics were computed without using any quality restrictions. It was found that such restrictions did not affect the daily and monthly validation results significantly.

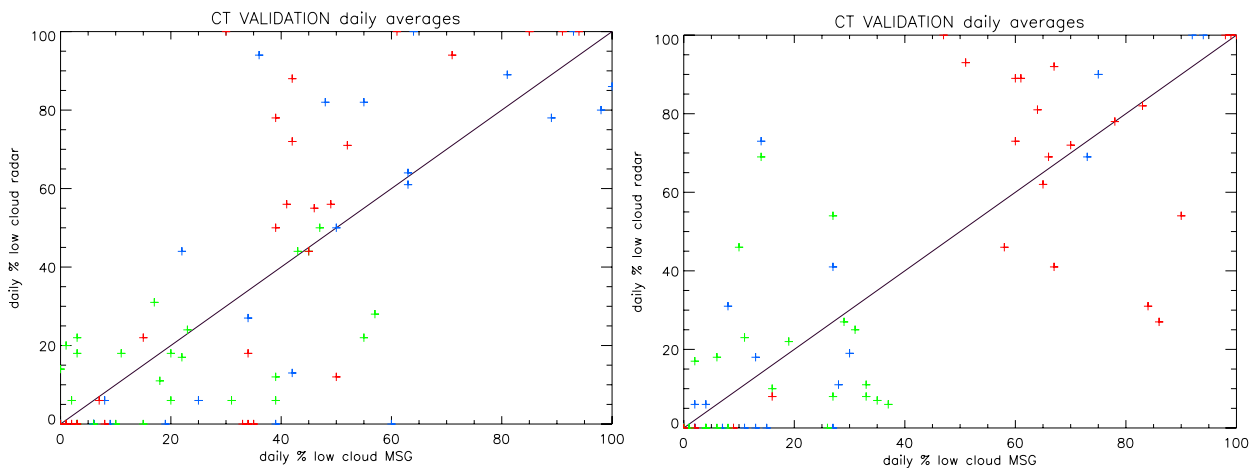
## 4.2 Results

Table 4.1 shows the summarized results for all individual comparisons for the two radar sites and using the two different vertical separation approaches. We notice that results are very similar for the two observation sites. In about two third of the cases the radar-derived and the MSG/SEVIRI-estimated cloud categories agree. The two different approaches for the vertical separation do not appear to affect results at all. In the following analysis, we have therefore chosen to use only the **Complex pressure level approach** since it is originally used as a basis for the MSG/SEVIRI CTY method.

Transferring the results into daily averages yields results as visualised in Figure 4.1 and as summarised in Table 4.2. The scatter in Figure 4.1 is quite considerable but we can see in Table 4.2 that the disagreement is mainly seen for Mid-level and High-level categories while the Low-level category has a higher level of agreement.

**Table 4.1** Percentage of matching cloud radar derived and MSG-derived CTY categories for the two different vertical separation approaches.

<b>Percentage of matching cloud radar and MSG CTY assignments</b>			
		<i>Radar CTY retrieval</i>	<i>Radar CTY retrieval</i>
		<b>Plain pressure level approach</b>	<b>Complex pressure level approach</b>
<b>Cabauw cloud radar</b>		66	67
<b>Chilbolton</b>	<b>cloud radar</b>	67	69



**Figure 4.1** Daily cloud type frequencies retrieved (%) from cloud radar data plotted against daily cloud type frequencies (%) retrieved from MSG CTY estimations. **Left**) Chilbolton cloud radar, **right**) Cabau cloud radar.

+ low level cloud category, + mid level cloud category, + high level cloud category.

	<b>Scientific Report</b> <b>Initial Validation of CM-SAF</b> <b>Cloud Products using</b> <b>MSG/SEVIRI Data</b>	Doc. No:	SAF/CM/DWD/SMHI/KNMI/SR/CLOUDS/1
		Issue:	1.0
		Date:	23 March 2005

**Table 4.2** Linear correlation coefficient ( $R^2$ ), offset (for regression curve) and RMS error for daily cloud radar/MSG CTY frequencies.

	Low-level clouds			Mid-level clouds			High-level clouds		
	Daily CTY frequencies			Daily CTY frequencies			Daily CTY frequencies		
	$R^2$	offset %	RMS	$R^2$	offset %	RMS	$R^2$	offset %	RMS
<b>Cabauw cloud radar</b>	0.8	0	16	0.2	10	10	0.7	12	25
<b>Chilbolton cloud radar</b>	0.8	-1	23	0.6	6	15	0.8	-1	25

**Table 4.3** Comparison of cloud radar retrieved monthly cloud frequencies and MSG retrieved monthly cloud frequencies

	Low-level clouds		Mid-level clouds		High-level clouds	
	Monthly CTY frequencies		Monthly CTY frequencies		Monthly CTY frequencies	
	Cloud radar %	MSG %	cloud radar %	MSG %	cloud radar %	MSG %
<b>Cabauw cloud radar</b>	22	29	16	14	62	57
<b>Chilbolton cloud radar</b>	41	40	20	19	39	41

Finally, if looking at the mean monthly results in Table 4.3 results are naturally improving through the smoothing of the results through the averaging procedure. Nevertheless, it is encouraging here to see a very good agreement with only a few percentage units in the difference between the cloud radar and MSG/SEVIRI monthly averages.

### 4.3 Summary of CTY validation results

An attempt to validate the CTY product using detailed information about cloud layer occurrence and cloud layer altitudes provided by cloud radar information has been carried out using data from a period covering one month (15 April – 14 May 2004). A transfer of initial cloud height information from cloud radars into corresponding cloud top temperature and cloud pressure values has enabled the creation of a set of cloud type categories that could be compared to the

	<b>Scientific Report</b> <b>Initial Validation of CM-SAF</b> <b>Cloud Products using</b> <b>MSG/SEVIRI Data</b>	Doc. No: <b>SAF/CM/DWD/SMHI/KNMI/SR/CLOUDS/1</b> Issue: <span style="float: right;"><b>1.0</b></span> Date: <span style="float: right;"><b>23 March 2005</b></span>
---	--	--

MSG/SEVIRI CTY product. Results show a considerable scatter for individual comparisons where about two third of the cases show agreement between cloud radars and the MSG/SEVIRI CTY categorisation. However, for the monthly average the difference in the respective occurrences of the cloud categories show small values (less than 8 %).

## 5 VALIDATION OF THE CLOUD TOP PRODUCT (CTH/CTP/CTT)

The CM-SAF MSG/SEVIRI Cloud Top retrievals are generated using the latest versions of the EUMETSAT Nowcasting Satellite Application Facility (SAFNWC) processing schemes. The NWC-SAF MSG/SEVIRI CTTT (Cloud Top Temperature and Height) product is described in detail in the corresponding scientific user manual (SAFNWC SUM/1, 2004). The scope of this validation activity is to outline the quality of one of the components of the CM-SAF cloud top products; the MSG/SEVIRI cloud top height product (CTH). Since the three components basically represent only different ways of expressing the product (not different methods), it is considered sufficient here to study only one of the components. However, in this context it must be added that the conversion between the components as well as the fundamental product definition relies to a great extent on the quality of ancillary data sets of vertical temperature and humidity profiles (in the CM-SAF taken from initial profiles from the GME NWP model). The CM-SAF implementation of this product is described further in CM-SAF UMP(2005).

One month of quasi-continuous cloud radar measurements from the Chilbolton (U.K.) and the Cabauw (The Netherlands) ground stations were analysed for inter-comparison with the MSG/SEVIRI CTH product. Hourly cloud top estimations as well as daily and monthly CM-SAF average products are compared to corresponding cloud radar retrievals. In addition, an inter-comparison between MSG/SEVIRI CTH retrievals, near simultaneous NOAA/AVHRR CTH retrievals and cloud radar data is presented as well as a reference to results from a recent CM-SAF Visiting Scientist study using LIDAR data for cloud top validation purposes. The validation covers the period April 15<sup>th</sup> to May 14<sup>th</sup> 2004.

### 5.1 Validation methods

In this section we shortly describe the methods used to compare MSG/SEVIRI CTH retrievals with cloud radar and NOAA/AVHRR CTHs.

#### 5.1.1 Cloud radar CTH retrievals

The cloud radar data were collected at the Cabauw (51.09 N, 4.93 E) and Chilbolton (51.10 N, 1.40 W) ground stations during the CloudNet campaign. A detailed description of the CloudNet campaign is provided in the next section (section 5), dealing with the CPH product. The cloud radar devices in Cabauw and Chilbolton were operated during the CloudNet campaign usually from 7:30 am to 5 pm. During the test period no major measurement discontinuities have been found.

The cloud radar data were processed to compute upper cloud boundaries using a software routine developed at KNMI. Generally, clouds and clear sky can be unambiguously detected by the cloud radar through the appearance of sharp boundaries. However, very high and optically thin cloud layers might not be detected by the cloud radar and hence the cloud radar retrieved CTH value does not always reflect the CTH of the uppermost cloud layer.

In order to compare the radar time series with the nearly instantaneous MSG/SEVIRI and NOAA/AVHRR measurements, the radar CTH retrievals were sampled over 30 minutes centred

	<b>Scientific Report</b> <b>Initial Validation of CM-SAF</b> <b>Cloud Products using</b> <b>MSG/SEVIRI Data</b>	Doc. No: <b>SAF/CM/DWD/SMHI/KNMI/SR/CLOUDS/1</b> Issue: <span style="float: right;"><b>1.0</b></span> Date: <span style="float: right;"><b>23 March 2005</b></span>
---	--	--

at the MSG/SEVIRI scene time. Since clouds move at different speeds and from different directions depending on the weather situation, one would ideally change the size of the satellite pixel area and the corresponding time window for the ground-based data depending on each situation. However, from both a technical and a scientific point of view this is a too demanding task and therefore the satellite pixel area and the time window were chosen with fixed sizes. The 30 minutes time window has been found to be optimal for satellite/ground device inter-comparisons in a previous validation study (Trolez et al., 2005).

For each cloud radar sample (15 and 30 seconds for Cabauw and Chilbolton, respectively), one CTH value is derived as at the transition between the uppermost detected cloud layer and the clear sky. These CTH retrievals are averaged over a 30-minute time window resulting in a common CTH value referred to as 'mean cloud radar CTH value'. Due to the fact that cloud decks are not necessarily continuous in a 30 minutes time window, additional information about the CTH variation in the time window is provided by means of minimum and maximum CTH.

Daily and monthly CTH averages were produced by calculating averages from continuous 30-minute CTH cloud radar data.

**5.1.2 MSG/SEVIRI and NOAA/AVHRR CTH retrievals**

For the MSG/SEVIRI and cloud radar CTH inter-comparison, hourly MSG/SEVIRI scenes from April 15<sup>th</sup> to May 14<sup>th</sup> 2004 were selected. Hourly MSG/SEVIRI data were chosen, because this is the chosen temporal resolution of the basic MSG/SEVIRI data set used in the CMSAF. In total, 446 MSG/SEVIRI cloud top estimations and corresponding cloud radar data sets were available for this validation study. Among those, 236 cases were available for the Chilbolton site and 210 for the Cabauw site.

MSG/SEVIRI CTH pixels were selected in 20 x 20 km pixel boxes centred on the position of the ground radar station to account for broken cloud situations and geometric dislocations. Different pixel boxes (5 km, 15 km, 20 km, 30 km) were tested and it was found that the CTH retrievals averaged over a 20 km pixel box shown the best agreement, in terms of minimum standard deviation of differences in CTH between ground radar and MSG/SEVIRI.

The choice of this quite large spatial window reflects the need to compensate for both the high temporal variability of the cloud decks that sometimes is found as well as for significant geometric dislocations. Concerning the first effect, it is clear that if trying to match instantaneous measurements in situations with high temporal cloud altitude variability one is likely to find a large scatter in the results. For the second effect (the parallax effect), it is clear that due to the viewing geometry of the MSG/SEVIRI sensor, a 10 km high cloud deck is shifted approximately 15 km to the North at latitude 50 N (a latitude representative for both radar sites) in the resulting SEVIRI scenes. This means that a direct comparison at pixel resolution will not be appropriate for mid- and high-level clouds.

Since the MSG/SEVIRI cloud top product is derived in two different ways, depending on if the cloud is labelled as opaque or semi-transparent/fractional (see SAFNWC SUM/1, 2004), a study of the results for these two different categories have also been included. Beside the average and maximum CTH value, results from semi-transparent or opaque cloud categories are compiled using the CTH product flag. Here, each case has been labelled into either of the two categories if more than 50 % of the box pixels are flagged as 'semi-transparent' or 'opaque'. For the Cabauw test site 68 pixel boxes were assigned as semi-transparent, while for the Chilbolton test-site only 23 semi-transparent cases were detected.

	<b>Scientific Report</b> <b>Initial Validation of CM-SAF</b> <b>Cloud Products using</b> <b>MSG/SEVIRI Data</b>	Doc. No: <b>SAF/CM/DWD/SMHI/KNMI/SR/CLOUDS/1</b> Issue: <span style="float: right;"><b>1.0</b></span> Date: <span style="float: right;"><b>23 March 2005</b></span>
---	--	--

For the MSG/SEVIRI CTH cases where corresponding radar CTH retrievals were available, CTH retrievals were also averaged into daily and monthly values for climatological inter-comparisons. The MSG/SEVIRI CTH averaging was performed similar to the averaging algorithms currently implemented in the CM-SAF production chain (i.e., monthly averages are based on averaging of daily averages). To be noticed is that the standard CM-SAF CTH products (based on all available MSG/SEVIRI scenes in a month) could not be used here since the cloud radar measurements are not continuous (night measurements are missing).

The NOAA/AVHRR CTH retrieval above the ground station is performed in an approximately similar way as the MSG/SEVIRI CTH retrieval (see SAFNWC SUM/2, 2004). Due to the absence of the particular parallax viewing problem for NOAA/AVHRR, a slightly smaller pixel box size (9 x 9 km) centred on the ground stations was chosen. This pixel box size has been found to be optimal for NOAA/AVHRR ground device inter-comparisons in previous validation study (e.g. see Trolez et al. 2005). In total, 46 simultaneous MSG/SEVIRI, cloud radar and NOAA/AVHRR CTH estimations were identified for the Chilbolton site and 44 for the Cabauw site.

**5.2 Results**

The following two subsections discuss the MSG/SEVIRI and cloud radar CTH inter-comparison as well as the comparison between MSG/SEVIRI, cloud radar and NOAA/AVHRR CTHs.

**5.2.1 Comparison between MSG/SEVIRI and Cloud radar CTH values**

MSG/SEVIRI CTHs are plotted versus radar CTHs in Figure 5.1. Here is also visible the distinction between opaque cloud cases (green) and semi-transparent cloud cases (red). The corresponding correlation coefficients as well as RMS errors are listed in Table 5.1.

Figure 5.1 reveals a fairly good agreement between satellite retrievals and the cloud radar measurements for the majority of the cases. At the same time, it is also clear that there are many problematic cases that deviate considerably from the one-to-one line. This is also further illustrated by the lower panel in Figure 5.1 showing the large variability of cloud top heights that exists in many cases within the chosen time window. There is no doubt that the problems with the temporal and spatial matching of measurements explain to a great extent the large scatter in the results.

A particularly interesting feature in the results is that there is a tendency for the semi-transparent retrievals to overestimate cloud top heights and for the opaque retrievals to underestimate cloud top heights.

Regarding the overestimation for the semi-transparent retrievals we could suspect that this is at least partly due to limitations in the ability of the cloud radar to observe very high and optically thin clouds. Another possible explanation could be that high thin clouds to the south of the radar site could have been geographically mis-located over the radar position due to the parallax effect. Otherwise, due to the slanted geometric view, one would suspect that the MSG/SEVIRI measurements would offer a quite good detection capability for these clouds (see also the discussion below associated with Figure 5.3).



**Scientific Report**  
**Initial Validation of CM-SAF**  
**Cloud Products using**  
**MSG/SEVIRI Data**

Doc. No:  
**SAF/CM/DWD/SMHI/KNMI/SR/CLOUDS/1**  
 Issue: **1.0**  
 Date: **23 March 2005**

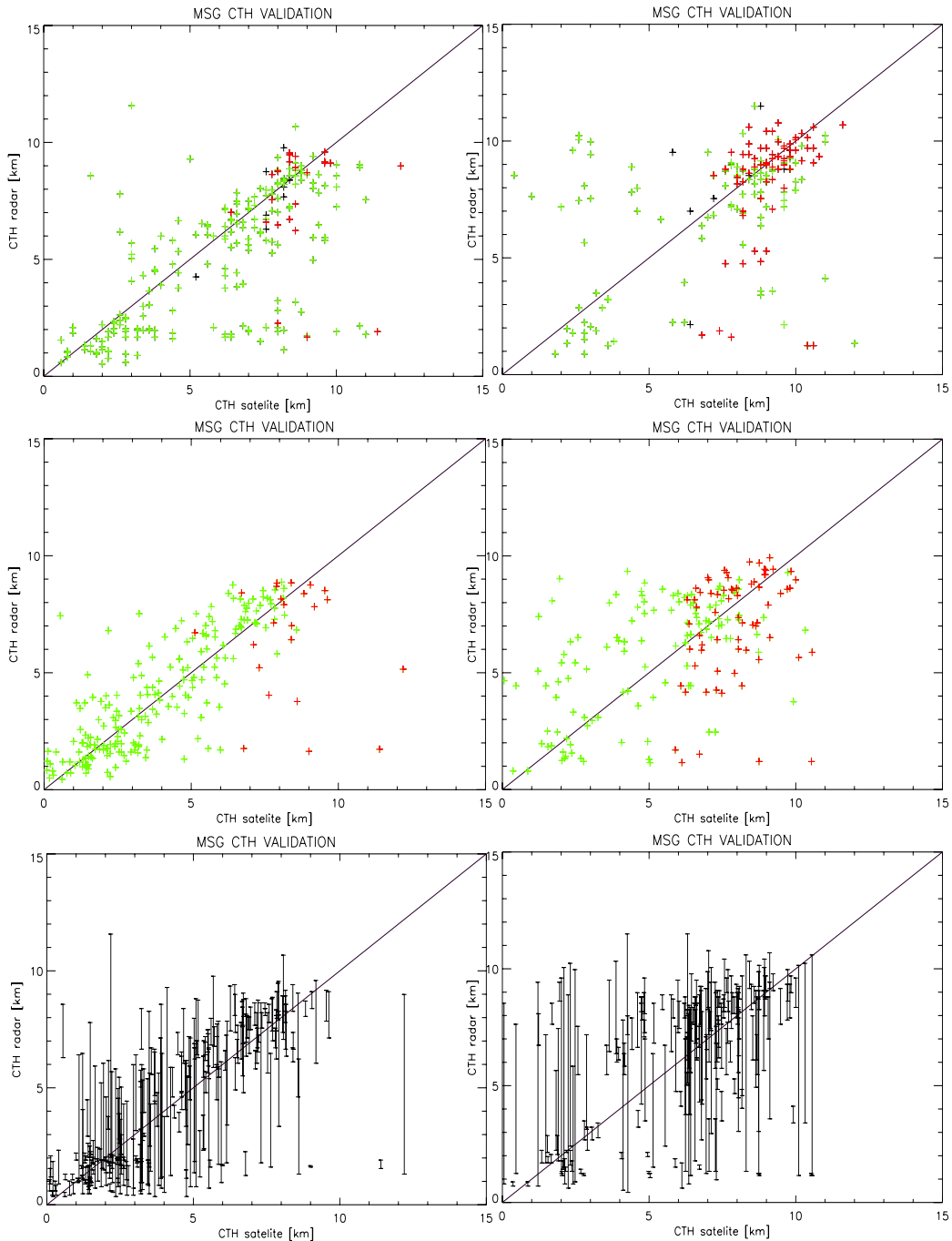


**Figure 5.1** MSG/SEVIRI cloud top heights (CTH) plotted against radar-retrieved CTHs. **Left)** Chilbolton ground station. **Right)** Cabauw ground station. **Upper)** Maximum CTH value in a 20 x 20 km MSG/SEVIRI box plotted against maximum cloud radar CTH in a 30 minute time window; red = semi-transparent, green = opaque, black = less than 50 % cloud coverage. **Middle)** Mean MSG/SEVIRI CTH plotted against mean radar CTH; red = semi-transparent, green = opaque, black = less than 50 % cloud coverage. **Lower)** Mean MSG/SEVIRI CTH plotted against minimum and maximum radar CTH values within the 30 minute time window.

	<b>Scientific Report</b> <b>Initial Validation of CM-SAF</b> <b>Cloud Products using</b> <b>MSG/SEVIRI Data</b>	Doc. No: <b>SAF/CM/DWD/SMHI/KNMI/SR/CLOUDS/1</b> Issue: <span style="float: right;"><b>1.0</b></span> Date: <span style="float: right;"><b>23 March 2005</b></span>
---	--	--

**Table 5.1** Linear correlation coefficient ( $R^2$ ) and RMS error for the cloud radar and MSG/SEVIRI CTH comparison. Max/mean MSG/SEVIRI: Maximum and mean cloud top height derived from a 20 x 20 km MSG/SEVIRI box centred over the cloud radar site. Max/mean radar: Maximum and mean CTH detected by the radar device in a 30-minute time window centered at the satellite acquisition time.

		max MSG/SEVIRI versus max radar		mean MSG/SEVIRI versus mean radar	
		$R^2$	RMS [m]	$R^2$	RMS [m]
<b>Cabauw radar</b>	<b>cloud</b>	0.43	2837	0.52	2441
<b>Chilbolton radar</b>	<b>cloud</b>	0.64	2560	0.78	1715

Regarding the indicated tendency of an underestimation of cloud heights for the opaque cloud group, one could suspect that this represents the cases where we have multiple cloud layers and where the uppermost layers are still detectable for the cloud radar. It is well known that if we have a semi-transparent cirrus clouds overlying an optically thick low- or mid-level water cloud the MSG/SEVIRI (and also the corresponding NOAA/AVHRR) cloud type determination will most often label these clouds as opaque and not as semi-transparent. Consequently, the infrared brightness temperatures used by the opaque CTH method are then composed by contributions from both high-level and low-level cloud layers. The CTH result will thus give a value that lies somewhere between the altitudes of the upper and lower level clouds, thus yielding an underestimation of the highest cloud heights.

Despite the indicated tendencies for the opaque method, it is also clear that we can also find quite a large number of cases where the opaque estimation gives an overestimation. Also here we can suspect that the problems in correctly matching satellite measurements and cloud radar measurements in time and space will partly contribute.

From Table 5.1 we find that for the mean CTH estimations we have a better agreement than for the maximum height estimations. The correlation coefficient is here 0.78 for Chilbolton and 0.52 for Cabauw. The rather high RMS errors in both cases indicate that the scatter in the results is considerable. However, it is clear from Figure 5.1 that much of this is caused by a relatively small amount of extreme outliers.

If instead transferring the results to daily and monthly averages (i.e., to the core CM-SAF products), a substantial part of the variability is naturally averaged out. Figure 5.2 and Table 5.2 shows the results for the daily and monthly averages.

We can still see some scatter in the results but the average values show a mean difference (bias) of only about -150 meters which is encouraging. Consequently, there is no sign of a systematic large error in the CTH retrievals which would have been serious for the use in climate applications.



**Scientific Report  
Initial Validation of CM-SAF  
Cloud Products using  
MSG/SEVIRI Data**

Doc. No:  
**SAF/CM/DWD/SMHI/KNMI/SR/CLOUDS/1**  
Issue: **1.0**  
Date: **23 March 2005**

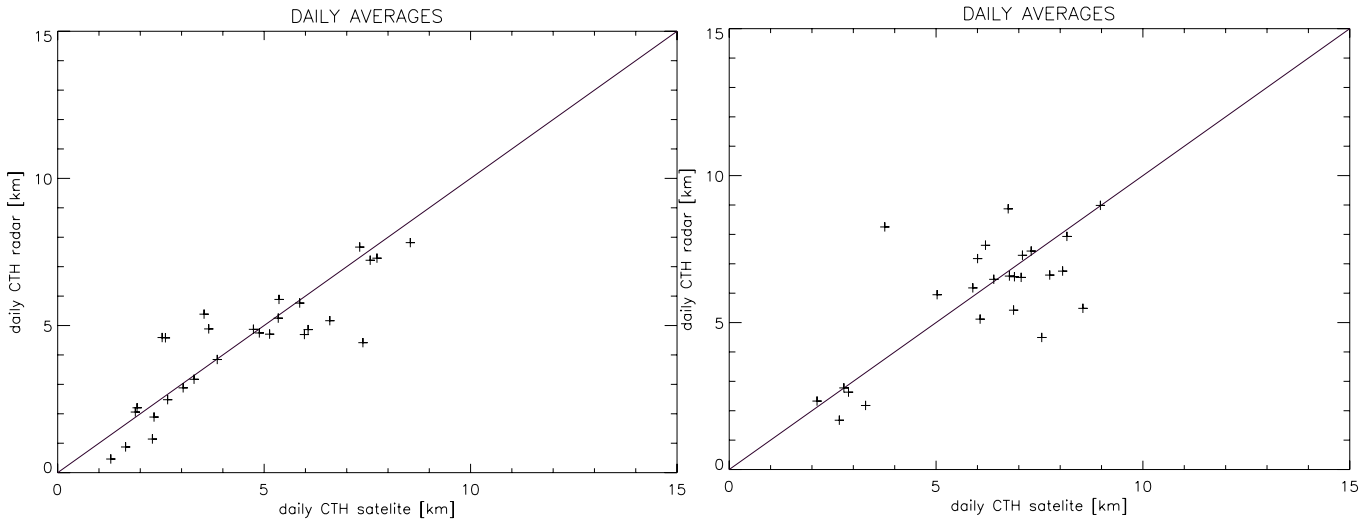


**Figure 5.2** Daily averaged MSG/SEVIRI cloud top heights (CTH) plotted against daily averaged radar retrieved CTHs. **Left)** Chilbolton ground station. **Right)** Cabauw ground station.

**Table 5.2** Linear correlation coefficient ( $R^2$ ) and RMS error for the daily cloud radar and daily MSG/SEVIRI comparison.

	daily mean MSG/SEVIRI versus daily mean radar		monthly mean MSG/SEVIRI versus monthly mean radar	
	$R^2$	RMS [m]	MSG/SEVIRI [m]	radar [m]
<b>Cabauw cloud radar</b>	0.73	1506	5893	6034
<b>Chilbolton cloud radar</b>	0.87	1060	4315	4466

### 5.2.2 Comparison between MSG/SEVIRI, cloud radar and NOAA/AVHRR CTHs

The results from the study on available cases with simultaneous MSG/SEVIRI, cloud radar and NOAA/AVHRR CTHs can be summarised by the following for the Chilbolton and Cabauw sites, respectively:

#### Chilbolton

- In 25 of 46 cases NOAA/AVHRR and MSG/SEVIRI agree within +/- 500 meter
- In 7 of 46 cases NOAA/AVHRR and MSG/SEVIRI retrievals differ more than +/- 500 meter but the MSG/SEVIRI retrieval still remains within the cloud radar maximum/minimum range
- In 14 of 46 cases NOAA/AVHRR and MSG/SEVIRI retrievals differ more than +/- 500 meter and the MSG/SEVIRI retrieval is outside the cloud radar maximum/minimum range

	<b>Scientific Report</b> <b>Initial Validation of CM-SAF</b> <b>Cloud Products using</b> <b>MSG/SEVIRI Data</b>	Doc. No: <b>SAF/CM/DWD/SMHI/KNMI/SR/CLOUDS/1</b> Issue: <span style="float: right;"><b>1.0</b></span> Date: <span style="float: right;"><b>23 March 2005</b></span>
---	--	--

**Cabauw**

- In 18 of 44 cases NOAA/AVHRR and MSG/SEVIRI agree within +/- 500 m
- In 10 of 44 cases NOAA/AVHRR and MSG/SEVIRI retrievals differ more than +/- 500 m but the MSG/SEVIRI retrieval still remains within the cloud radar maximum/minimum range
- In 16 of 44 cases NOAA/AVHRR and MSG/SEVIRI retrievals differ more than +/- 500 m and the MSG/SEVIRI retrieval is outside the cloud radar maximum/minimum range

The linear correlation and the RMS error are also given for both sites in Table 5.3. It shows fairly reasonable correlation between the two retrieval methods but it is clear that there is quite a high variability in the different CTH estimations as indicated by the relatively high RMS values.

**Table 5.3** Linear correlation coefficient ( $R^2$ ) and RMS error for the NOAA/AVHRR and MSG/SEVIRI comparison. The max/min NOAA/AVHRR and MSG/SEVIRI refers to the maximum and mean cloud top height derived from 9 x 9 km (NOAA/AVHRR) or 20 x 20 km boxes (MSG/SEVIRI) centred around the corresponding cloud radar.

		max MSG/SEVIRI versus max NOAA/AVHRR		mean MSG/SEVIRI versus mean NOAA/AVHRR	
		$R^2$	RMS [m]	$R^2$	RMS [m]
<b>Cabauw radar</b>	<b>cloud</b>	0.78	2307	0.87	1528
<b>Chilbolton radar</b>	<b>cloud</b>	0.57	2547	0.76	1481

As a final comment to the cloud top height validation work it should be remarked that no in depth analysis of the outliers seen in e.g. Figure 5.1 and indicated by the high RMS values in Table 5.1, Table 5.2 and Table 5.3 has been possible. This will be one particularly important task for the validation work to be carried out for the next ORR V2 review.

**5.3 Additional results from other validation periods**

The previous sub-section indicated a fairly good agreement between NOAA/AVHRR and MSG/SEVIRI cloud top estimations. Further support to this view is found in Figure 5.3 showing a scatterplot of all cloud top temperature (CTT) retrievals from NOAA/AVHRR and MSG/SEVIRI during the month of October 2004. The alignment along the one-to-one line is remarkable even if the histogram reveals some differences. It is well known that the NOAA/AVHRR CTT retrieval for semi-transparent high clouds do not work (iteration method not converging) for a significant fraction of the cases which leads to some under-representation of the coldest CTT values which is clearly seen in the histogram.

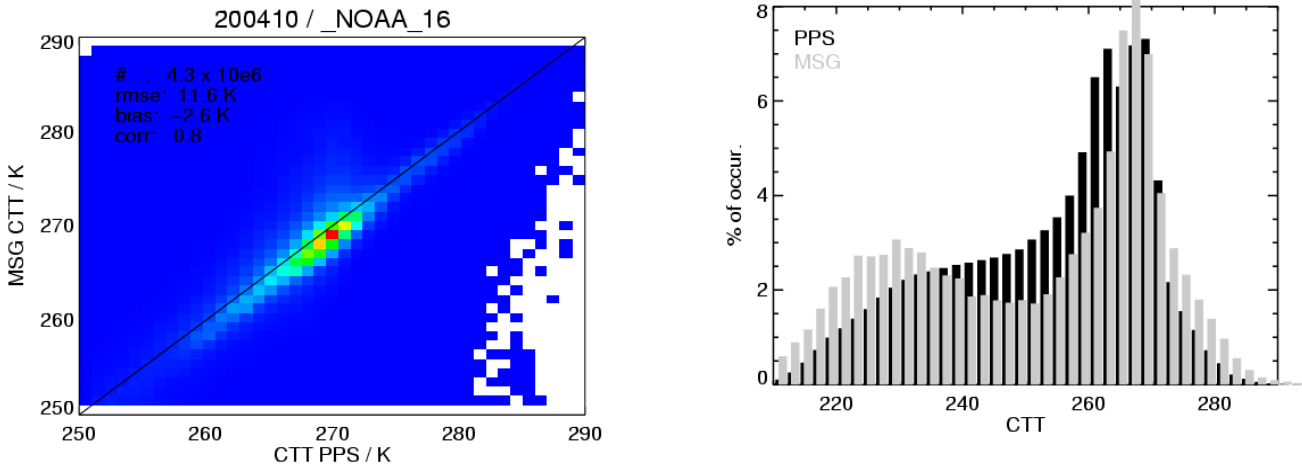


**Figure 5.3** *Left:* Scatterplot of all simultaneous CTT retrievals from MSG/SEVIRI and NOAA/AVHRR (PPS – although, here only showing results from NOAA-16) during the month of October 2004. *Right:* Corresponding CTT histogram for the two methods (MSG and PPS).

Finally, it is appropriate in this context to also show results from a recently finished CM-SAF Visiting Scientist study, focused on the validation of NOAA/AVHRR cloud top retrievals of semi-transparent clouds (Trolez et al., 2005). This study included also a limited comparison to MSG CTH retrievals and the result is shown in Figure 5.4.

When interpreting this figure it should be made clear that low- and mid-level water clouds attenuate the LIDAR signal in a much more significant way compared to what is the case for the cloud radar signal. Consequently, the results in Figure 5.4 show only a sub-set of selected cases where cloudiness below 4000 meter’s altitude has been minimised in order to focus on the high-level cloud cases. The cases were selected during the period between March-July 2004 for the SIRTALIDAR site in Palaiseaux, Paris. Thus, practically all cases show high-level clouds, interpreted either as semi-transparent or opaque. A larger number of semi-transparent cases are seen in the SEVIRI data compared to the corresponding NOAA/AVHRR retrievals. This gives an indication of a somewhat higher sensitivity to the existence of thin cirrus clouds for the MSG/SEVIRI algorithm. The results for this category also show a better performance compared to the semi-transparent category for NOAA/AVHRR. However, for the opaque retrieval results seem much worse than the LIDAR value (partly valid also for the NOAA AVHRR retrieval). This raises the question of if there are parallax problems or other geolocation problems in the SEVIRI data or if it could be explained by special LIDAR characteristics (e.g. a higher sensitivity of upper-level thin cloud layers in case of multi-layer situations). For more details about this study, the reader is referred to Matthieu et al. (2005).

#### 5.4 Summary of CTH/CTP/CTT validation results

The cloud top validation study has shown that it is difficult to find a very good agreement between MSG/SEVIRI cloud top estimations and corresponding cloud radar and LIDAR retrievals. There are many possible reasons for this, and among those the problems with the temporal and spatial matching of the two measurements/estimations probably explain most of this variability. Although, encouraging is that when averaging results into daily and monthly averages correlations are quite high (approximately 0.80) and biases are small (approximately -150 meters). The agreement

between the MSG/SEVIRI and NOAA/AVHRR cloud top retrievals appear also to be fairly high and with only small biases (e.g., some under-representation of the coldest temperatures in NOAA/AVHRR retrievals).

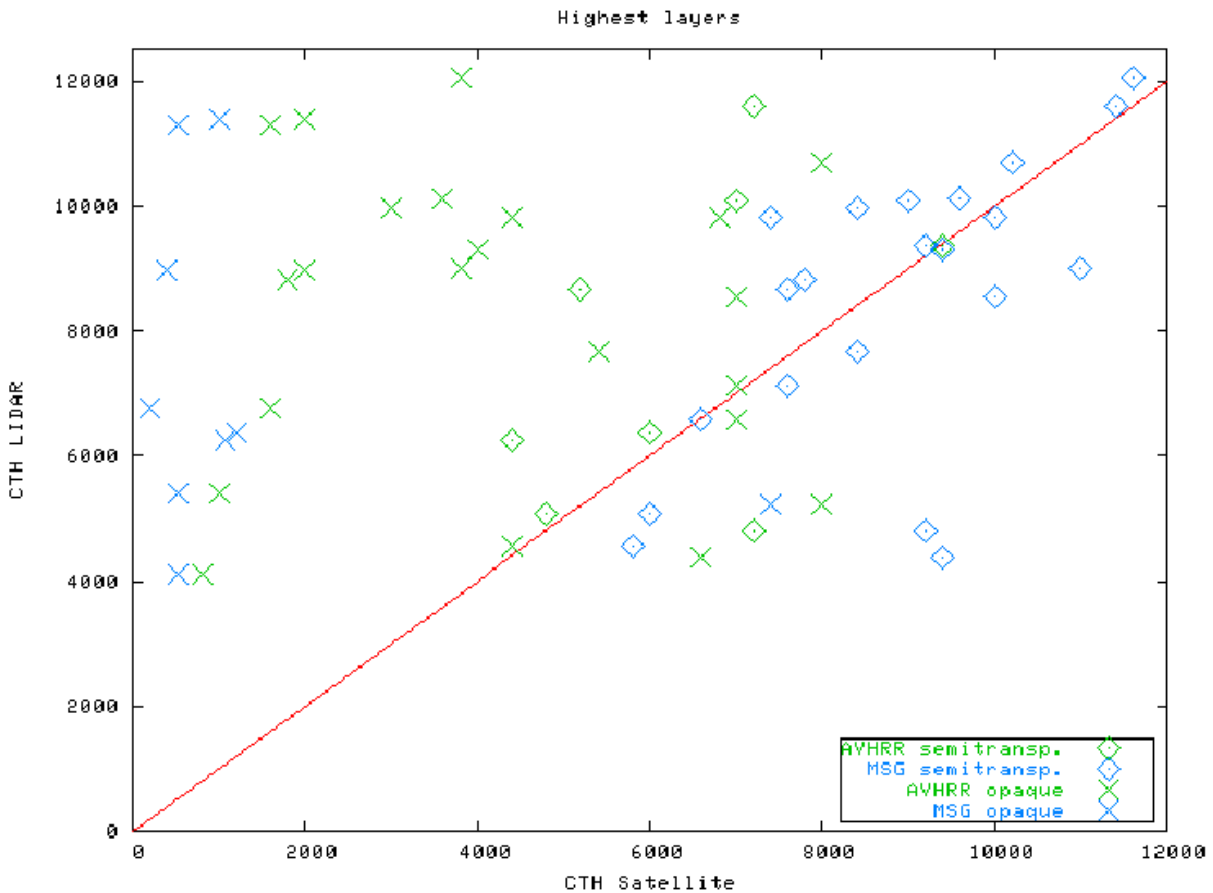


**Figure 5.4** Results of the inter-comparison between simultaneous AVHRR and SEVIRI CTH retrievals using the highest layer approach (i.e., highest LIDAR layer is compared to the highest satellite layer) for the SIRTA LIDAR site in the period March-July 2004 (see Trolez et al., 2005).

## 6 VALIDATION OF THE THERMODYNAMIC CLOUD PHASE PRODUCT (CPH)

The CPH product gives information on the cloud thermodynamic phase. The product is retrieved using reflectances from the 0.6 and 1.6  $\mu\text{m}$  SEVIRI channels. Further, retrieval of the ice phase is given an additional evaluation by means of a cloud top temperature check. A more detailed description of the product and the used methodology is given in CM-SAF UMP(2005).

### 6.1 Validation method

The MSG cloud thermodynamic phase (CPH) was retrieved for the satellite pixel that collocated best with the observation stations of Cabauw and Chilbolton. The area represented by the

	<b>Scientific Report</b> <b>Initial Validation of CM-SAF</b> <b>Cloud Products using</b> <b>MSG/SEVIRI Data</b>	Doc. No: <b>SAF/CM/DWD/SMHI/KNMI/SR/CLOUDS/1</b> Issue: <span style="float: right;"><b>1.0</b></span> Date: <span style="float: right;"><b>23 March 2005</b></span>
---	--	--

satellite pixel is about 18 km<sup>2</sup>. The product output values are liquid water or ice. Satellite retrieved CPH values are compared to CPH values derived from a cloud radar and lidar combination. This method was described in detail by Hogan *et al.* (2003). A time window with duration of 10 minutes centred on the slot time of the MSG satellite was chosen to be more or less representative for the horizontal extent of the pixel area. Further, only cases with a cloud cover from satellite greater than 80%, derived from 9 pixels centred on the validation station, were included in the validation.

The radar/lidar method, based on radar/lidar samples every 15 (Cabauw) or 30 seconds (Chilbolton), yields information on the cloud phase (water or ice). The horizontal resolution is a few tens of meters and is thus much finer than the satellite pixel resolution. As a result of this, small-scale effects like e.g. small patches of cirrus over a water cloud can play a role. In order to minimise these effects a threshold for each of the phases is set to label the time window period. That is, one of the two phases should be detected by the radar/lidar method for at least 80% (=8 minutes) of the time window period to yield a distinct phase.

## 6.2 Results

From the collocated dataset of distinct cloud phases for both validation stations, a contingency table was made. The table consists of four categories ([satellite water-ground water](#), [satellite water-ground ice](#), [satellite ice-ground water](#) and [satellite ice-ground ice](#)). In Table 6.1 results of this categorization are shown in absolute numbers.

**Table 6.1** Contingency table of collocated cloud thermodynamic phase for Cabauw (a) and Chilbolton (b). Included are cases with satellite cloud cover > 80% and optical thickness  $\tau > 0$ . Cabauw:  $n=205$ , Chilbolton:  $n=217$ .

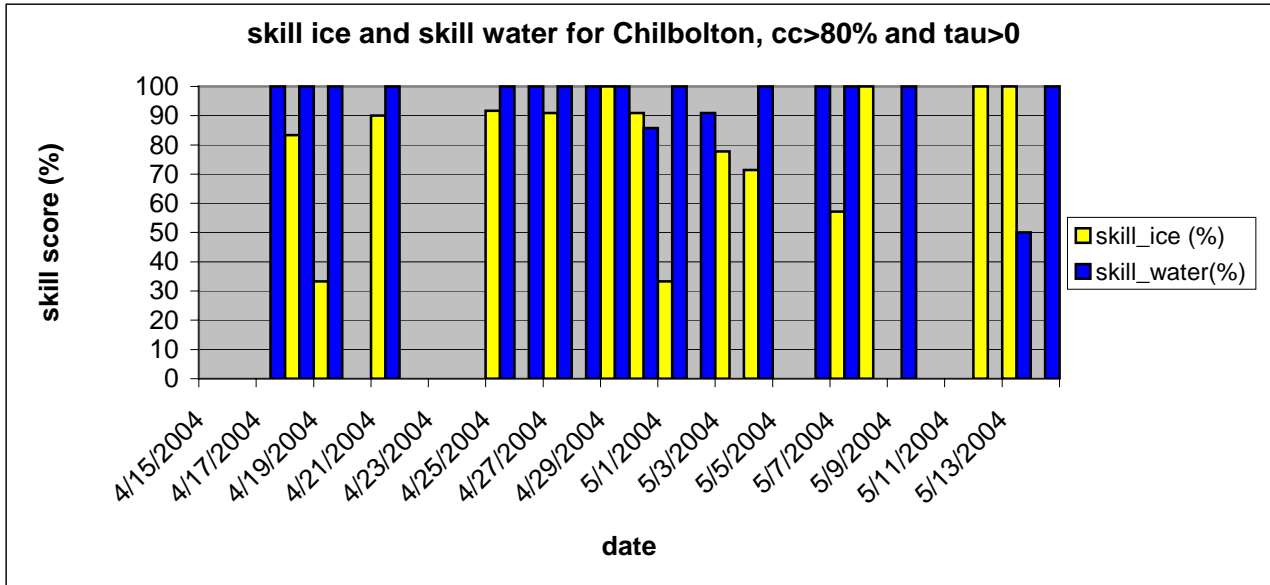
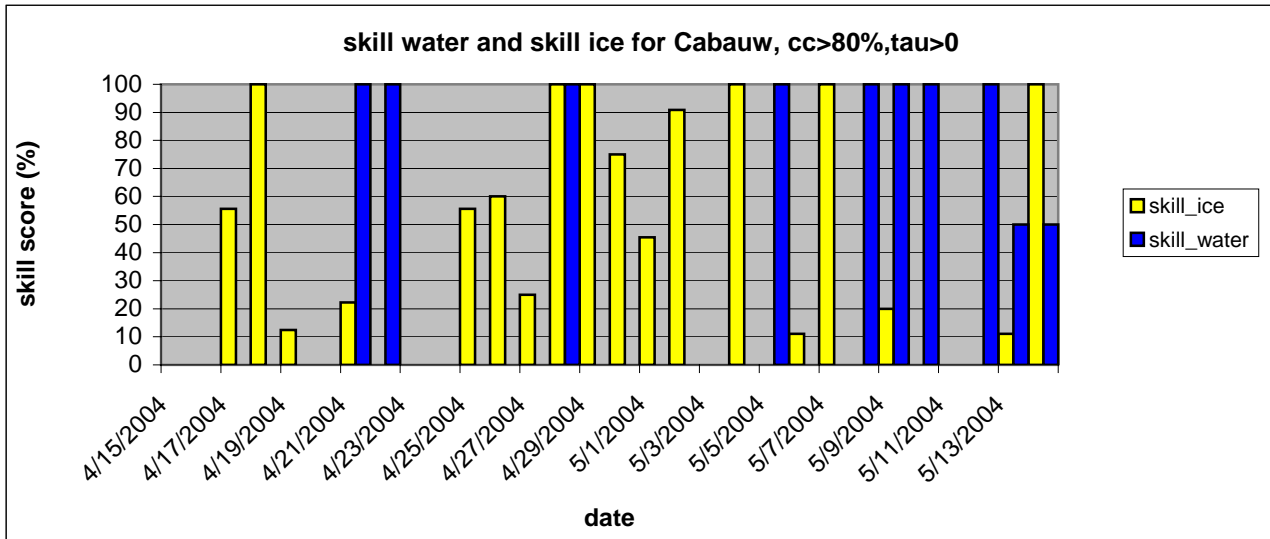
Cloud phase	Lidar/radar_water	Lidar/radar_ice
MSG_water	34	76
MSG_ice	4	91
(a)		
Cloud phase	Lidar/radar_water	Lidar/radar_ice
MSG_water	91	27
MSG_ice	9	90
(b)		

As one can see from Table 6.1a, the number of “correct” satellite retrievals for water and ice at Cabauw are 34 and 91 respectively. Taking the cloud phase from ground as a reference, we can define a skill parameter for the satellite water and ice retrieval by dividing the number of correct satellite phase retrievals by the total number of the phase derived from lidar/radar measurements, thus yielding a skill for the satellite ice phase retrieval of 0.55 (=91/167). In other words, just over half of the satellite ice phase retrievals in the Cabauw dataset are correct. In a similar way, the skill for the satellite water phase retrieval was calculated, resulting in a value of 0.89.

The results for Chilbolton are to a large extent the same for the water phase retrieval, having a skill value of 0.91. The skill score for the ice phase retrieval has a higher value than at Cabauw (0.77). Merging the two datasets into one results in a skill score of 0.64 for the ice phase and 0.91

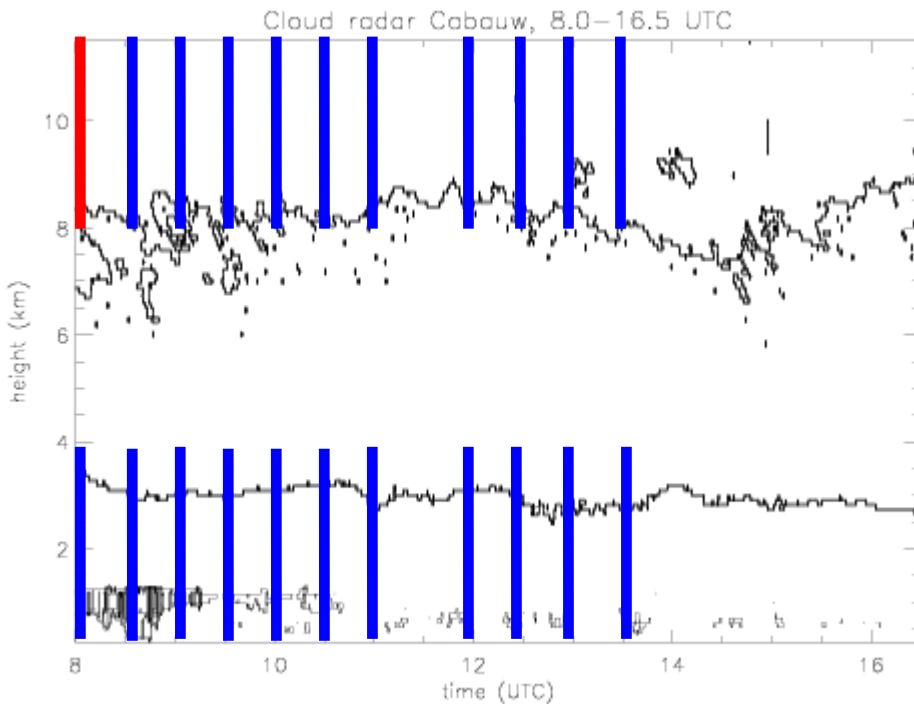
for the liquid phase (n=422). This high skill value might be artificially high due to the large number of satellite water retrievals: 54% of all retrievals for Cabauw and Chilbolton are retrieved as water, whereas only 33% of the ground retrievals result in the liquid phase, thus giving a difference of 21%.

Figure 6.1 shows histograms of the water and ice skill for each day. From the figure it can be seen that for Cabauw and Chilbolton the skill in water phase is 100% for almost all days. For the ice phase skill, at both stations there is a relatively high variability throughout the validation period. If a skill score of 50% is taken as a low quality limit, at Cabauw seven and at Chilbolton two days do not fulfil this criterion.



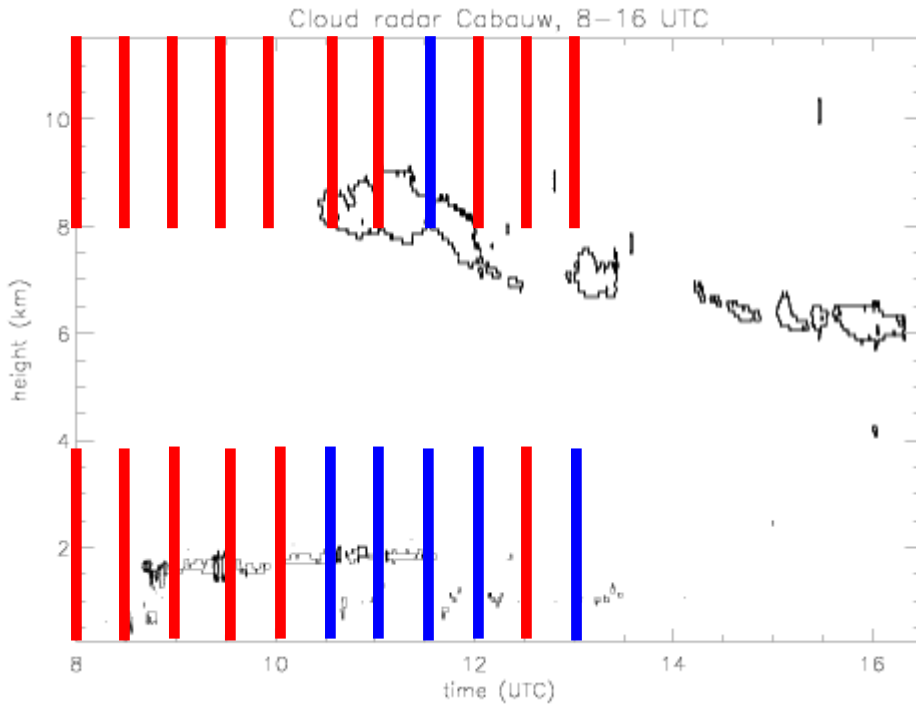
**Figure 6.1** Daily skill of the satellite water and ice phase retrieval for Cabauw (upper graph) and Chilbolton (lower graph). Cloud cover and optical thickness thresholds as in Table 6.1.

Figure 6.2 shows cloud radar data at Cabauw of May 2<sup>nd</sup> 2004. The scene was dominated by a thick package of midlevel and high-level clouds. From 8:00 UTC till about 10:00 UTC, also some stratocumulus was present as a low cloud layer. The freezing level, taken from sounding data of de Bilt (about 35 km north-east of Cabauw), was at about 2000 m and the cloud base temperature of the upper cloud layer was about 268 K. Satellite derived optical thickness values were mostly in the range of 4-8. As can be seen from the cloud phase retrievals from METEOSAT-8 and lidar/radar, there was a very good agreement with 10 out of 11 correct retrievals.



**Figure 6.2** Cloud radar at Cabauw, May 2<sup>nd</sup> 2004, 8:00-16:30 UTC. Cloud thermodynamic phase retrievals are superposed for MSG (upper bars) and the lidar/radar algorithm (lower bars), with a red bar representing water and a blue bar representing ice.

From the cloud radar plot in Figure 6.3, showing data of May 9<sup>th</sup> at Cabauw, it can be seen that at this day two types of cloud were present. From 8:00 UTC to about 11:30 UTC thin (strato) cumulus clouds were present. From 10:30 UTC there were cirrus clouds with a patchy structure. Cloud top temperature from cloud radar can also be divided into these two categories. For the first type of cloud, cloud top temperatures around the freezing point (273 K) were derived by cloud radar, decreasing to 225-240 K after appearance of the cirrus clouds. The satellite CPH retrievals were correct for the first time period (5 out of 5), however for the cirrus cases only 1 out of 5 satellite retrievals did yield the ice phase. This low skill score might be attributed to the low optical thickness values of the cirrus clouds (satellite retrieved values were generally in the range of 2-6). This may lead to semi-transparency effects and thus too high values of satellite retrieved cloud top temperatures, despite the better detection ability for high clouds as a result of the slanted view of MSG. As a result of the high cloud top temperature values, a cloudy pixel initially identified as of the solid phase may subsequently be labelled as water cloud.



**Figure 6.3** Cloud radar at Cabauw, May 9<sup>th</sup> 2004, 8:00-16:30 UTC. Cloud thermodynamic phase retrievals are superposed for MSG (upper bars) and the lidar/radar algorithm (lower bars), with a red bar representing water and a blue bar representing ice.

### 6.3 Summary of CPH validation results

Results of the MSG/SEVIRI CPH retrieval algorithm were compared with results of a lidar/radar algorithm by means of a categorisation (satellite water-ground water, satellite water-ground ice, satellite ice-ground water and satellite ice-ground ice). Taking the cloud phase retrieved from ground measurements as reference; from these four categories skill scores are derived for the MSG water and ice phase retrieval. The skill score for the MSG water and ice phase retrieval are 0.91 and 0.64 respectively. Skill scores for the ice phase retrieval are low for cases with semi-transparent clouds. As a result of the high number of water retrievals of the MSG algorithm (54% of the total) compared to the lidar/radar algorithm (33% of the total), the skill score of the MSG water phase retrieval might be artificially high. Future CPH validation activities will concentrate more on multi-layer and semi-transparent cases.

## 7 VALIDATION OF THE OPTICAL THICKNESS PRODUCT (COT)

This product provides information on the Cloud Optical Thickness (COT) and, as an intermediate product, the cloud droplet effective radius for pixels that are flagged cloudy by the cloud detection test. The algorithm retrieves these products on the basis of 0.6 and 1.6  $\mu\text{m}$  channel data for NOAA-AVHRR and MSG/SEVIRI data.

The method to retrieve the cloud optical thickness utilizes solar reflected measurements at non-absorbing and absorbing wavelengths. The underlying principle of the method is that cloud

	<b>Scientific Report</b> <b>Initial Validation of CM-SAF</b> <b>Cloud Products using</b> <b>MSG/SEVIRI Data</b>	Doc. No: <b>SAF/CM/DWD/SMHI/KNMI/SR/CLOUDS/1</b> Issue: <span style="float: right;"><b>1.0</b></span> Date: <span style="float: right;"><b>23 March 2005</b></span>
---	--	--

reflectance at a non-absorbing channel in the visible wavelength region is primarily a function of the optical thickness, whereas the reflectance at a water or ice absorbing channel in the near infrared is primarily a function of cloud particle size (Nakajima and King, 1990). By combining the information of non-absorbing and absorbing channels it is possible to retrieve the droplet effective radius and the cloud optical thickness. Nakajima and Nakajima (1995) developed a method to retrieve cloud optical thickness and effective particle radius based on satellite channel radiances at 0.6, 3.7 and 10.8  $\mu\text{m}$ . The method used in the CM-SAF is based on the same principle. However, the CM-SAF method utilizes the 1.6  $\mu\text{m}$  near infrared channel (Jolivet, 2000, Roebeling *et al.*, 2003) instead of the 3.7  $\mu\text{m}$  channel.

## 7.1 Validation method

The validation of MSG/SEVIRI cloud optical thickness retrievals is based on ground-based pyranometer measurements. Pyranometers measure broadband hemispherical irradiance in the solar spectrum. Methods have been developed to relate pyranometer observations to narrowband cloud optical thickness. The principle of these methods is the unique relationship of transmitted solar radiation to cloud optical thickness. Radiative transfer calculations can be conducted to relate broadband irradiance observations to narrowband cloud optical thickness (Deneke, 2002). The cloud optical thickness is calculated for an imaginary plane-parallel homogeneous cloud layer that produces the same radiation field at the surface as the actual cloud layer. For the cloud microphysical properties a representative water (or ice) cloud has to be assumed with a given droplet size distribution, effective radius and effective variance.

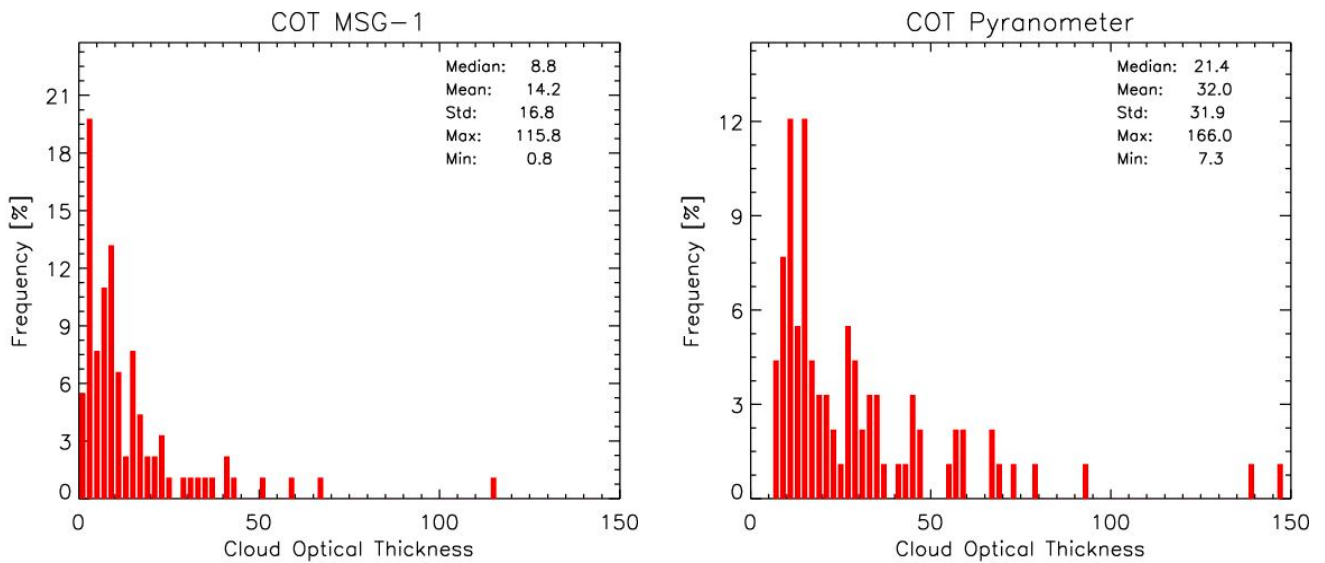
MSG- and pyranometer-derived cloud optical thickness values were compared for the period April 15<sup>th</sup> till May 31<sup>st</sup> 2004 for Cabauw, The Netherlands. Half hourly MSG-1 images were processed during daylight hours (8:00 – 16:30 UTC) for an area over central Europe, covering the CloudNET sites of Paris/Palaiseau (France), Chilbolton (UK) and Cabauw (The Netherlands). The pyranometer cloud optical thickness was derived with the approach proposed by Barnard and Long (2004), who give a simple empirical equation to approximate cloud optical thickness as function of the solar broadband irradiances. This approach is most closely satisfied for fully overcast skies. Therefore, cases of broken cloudiness cannot be considered. The difference between the transmission through the cloud and the transmission through the atmospheric layers above and below the cloud is ignored because we have no detailed information on vertical distribution of the atmosphere's optical properties. The MSG cloud optical thickness was extracted for the satellite pixel that collocated best with the Cabauw observation site (51.97°N, 4.93°E). The pyranometer cloud optical thickness values were calculated for the observations closest to the time that MSG-1 scans the Cabauw observation site, which is about 13 minutes after MSG-1 starts scanning on the southeast side of the Earth disk.

## 7.2 Results

Frequency distributions of pyranometer- and MSG-retrieved optical thickness values were analysed to make a statistical comparison of ground-based and satellite derived cloud optical thickness values. Figure 7.1 shows the comparison of MSG- and pyranometer-derived frequency distributions of cloud optical thickness for April 14th - April 30th 2004 (upper panel) and May 1st – May 31st 2004 (lower panel). For the two observation periods the frequency distributions of the individual instruments are very similar, which indicates that the dataset is large enough for a statistical analysis. The frequencies of cloud optical thickness of both instruments are log-normally distributed. The median values of MSG cloud optical thickness are about 8 and the minimum value is zero. With a median cloud optical thickness of about 20 the optical thickness

retrieved from pyranometer is significantly higher than the optical thickness derived from MSG. The minimum pyranometer optical thickness is about 6. This high minimum optical thickness results from the selection of completely overcast sky cases for the retrieval of pyranometer optical thickness. This selection can cause an overestimation of pyranometer optical thickness because the MSG optical thickness for these cases can be lower due to collocation errors and differences in the sampling area.

14 – 30 April 2004



1- 31 May 2004

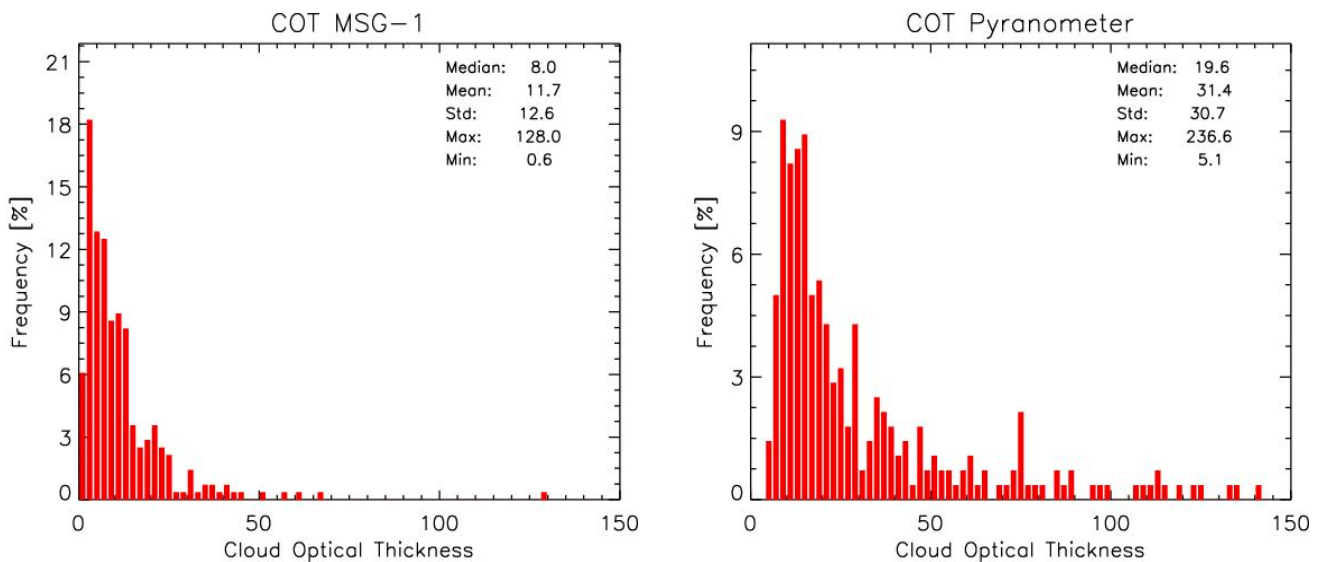


**Figure 7.1** Frequency distributions of MSG-1 (Meteosat-8) and pyranometer-derived cloud optical thickness for Cabauw, The Netherlands. The upper two distributions were made for April 14<sup>th</sup> till April 30<sup>th</sup> 2004, the lower two distributions for May 2004.

Figure 7.2 shows the differences between cloud optical thickness retrieved from pyranometer and MSG. The figure illustrates that for ~50% of the observations the differences between pyranometer and MSG cloud optical thickness are within the range of -8 to 8. The maximum frequency of differences is observed at about 8. However, for a considerable number of observations the pyranometer cloud optical thickness values are higher than those from MSG with maximum differences up to 200. For both observation periods the standard deviation of difference is about 28.

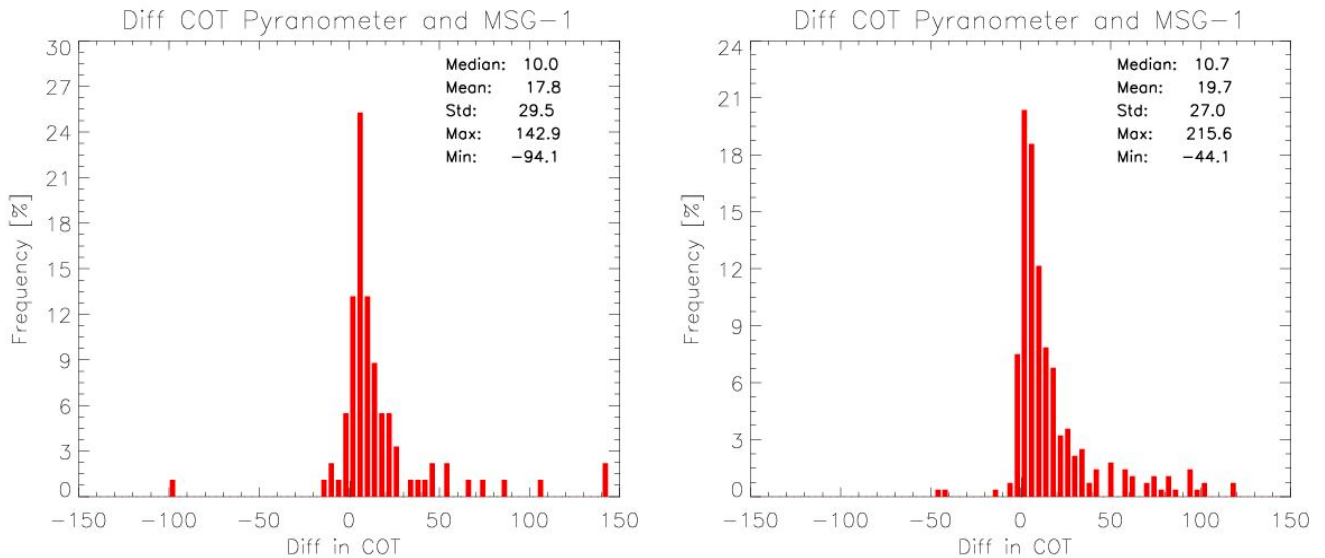


**Figure 7.2** Frequency distributions of differences between pyranometer and MSG-1 (METEOSAT-8) derived cloud optical thickness for April 14<sup>th</sup> till April 30<sup>th</sup> 2004 (left panel) and May 2004 (right panel) for Cabauw, The Netherlands.

The comparison between pyranometer and MSG optical thickness presented in Figure 7.3 shows a large scatter. Part of the scatter most likely originates from spatial mismatch between ground-based and satellite observations. The spatial resolution of MSG images over The Netherlands is about 3\*6 km. The representativity of the pyranometer observations depends on the altitude of the cloud base and the distribution of clouds around the ground-based station. This means that the satellite and the ground-based cloud optical thickness values are likely to represent somewhat different cloud scenes. However, their statistical distributions are expected to be more consistent. Table 7.1 summarises the comparison of pyranometer and MSG cloud optical thickness. The absolute differences between the mean pyranometer and MSG-derived optical thickness are large with pyranometer cloud optical thickness values being 17.8 and 19.7 higher for April 14<sup>th</sup> till April 30<sup>th</sup> 2004 and May 2004 respectively. The median differences are slightly lower with a value of about 10. The observed differences cannot entirely be explained by collocation or sampling errors. Part of the observed differences can be dedicated to the sensitivity of the pyranometer cloud optical thickness retrievals to fluctuations in cloud and atmospheric properties. The empirical relationship of Barnard and Long (2004) does not consider variations in solar zenith angle, aerosol optical thickness, cloud particle effective radius and water vapor and ozone concentration. Moreover, the empirical relationship is based on observations of 3 ARM sites (Alaska, Southern Great Planes and Papua New Guinea) and was never tested for Cabauw. Finally, there are two sources of error that are not included in the retrieval because they are

difficult to measure from the ground i.e., the fractions of ice and water in the cloud and the inhomogeneities within the cloud and in cloud cover.

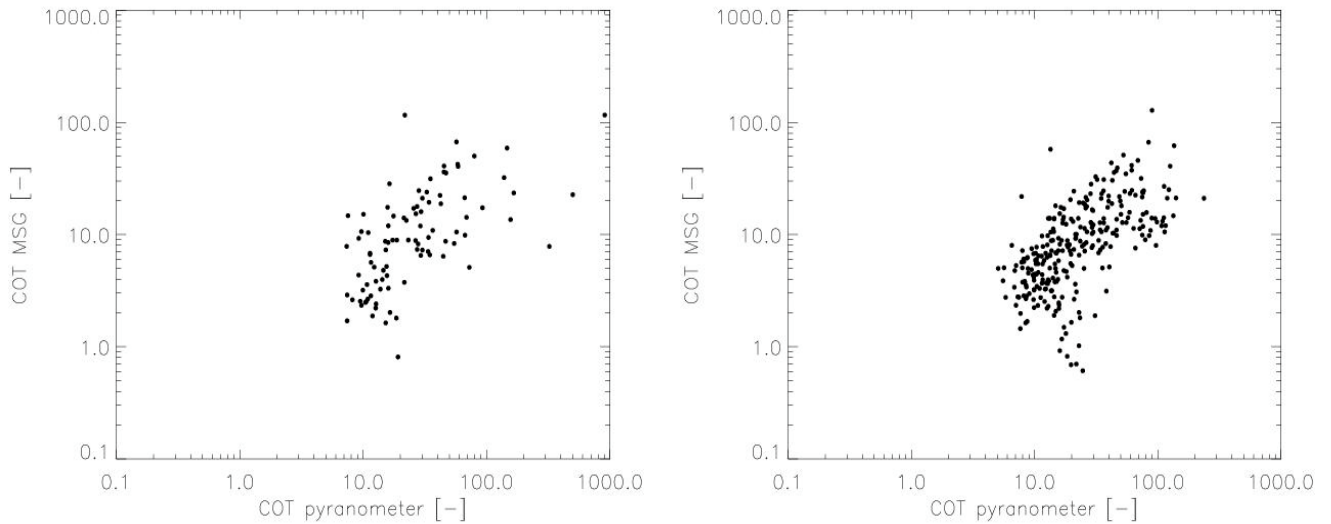


**Figure 7.3** Scatter plots of pyranometer and MSG-derived COT for Cabauw, The Netherlands. Left panel: April 14<sup>th</sup> till April 30<sup>th</sup> 2004, right panel: May 1<sup>st</sup> till May 31<sup>st</sup> 2004.

**Table 7.1** Summary of comparison of MSG and pyranometer derived Cloud Optical Thickness

	Median COT MSG	Median COT Pyranometer	Mean difference Pyr. - MSG	Std. of difference Pyr. - MSG
<b>14 – 30 April 2004</b>	<b>8.9</b>	<b>21.4</b>	<b>17.8</b>	<b>29.5</b>
<b>01 – 31 May 2004</b>	<b>8.0</b>	<b>19.6</b>	<b>19.7</b>	<b>27.0</b>

### 7.3 Summary of COT validation results

Results of the COT retrieval algorithm indicate that the MSG/SEVIRI cloud optical thickness values have smaller median and minimum values than the pyranometer retrieved values. The maximum frequency of differences between pyranometer and MSG-retrieved optical thickness is about 8, however differences up to 200 are observed. Part of the differences is caused by the selection criterion for the ground-based retrieval, which only allows completely overcast skies for the retrieval of pyranometer optical thickness. This may result in an overestimation of the pyranometer optical thickness. Other sources of error are mismatches in collocation and the sensitivity of the pyranometer retrieval algorithm to inhomogeneities in cloud and atmospheric properties. To minimise collocation errors, daily averages of MSG and pyranometer retrieved COT values were compared and this gave a correlation of about 0.85. This is significantly better

	<b>Scientific Report</b> <b>Initial Validation of CM-SAF</b> <b>Cloud Products using</b> <b>MSG/SEVIRI Data</b>	Doc. No: <b>SAF/CM/DWD/SMHI/KNMI/SR/CLOUDS/1</b> Issue: <span style="float: right;"><b>1.0</b></span> Date: <span style="float: right;"><b>23 March 2005</b></span>
---	--	--

than the correlation of the half-hourly observations of about 0.45. The current validation activity was done for completely overcast skies only; future validation studies should also include broken cloud fields.

## 8 VALIDATION OF THE CLOUD WATER PATH PRODUCT (CWP)

This product provides information on the Cloud Liquid Water Path (CLWP) given in  $\text{gm}^{-2}$ . The CLWP is calculated as a function of the Cloud Optical Thickness and the droplet effective radius estimate ( $r_{e(1.6 \mu\text{m})}$ ). Notice, however, that in most presentations of CM-SAF products this product is abbreviated as CWP (as in the section heading and in Table 1.1) for consistency with the naming convention for other products (three letter acronyms). However, in this section we will make use of the CLWP notation to clearly indicate that it is not treating the ice water path with the same accuracy (as commented further below).

The Cloud Liquid Water Path (CLWP) is derived from the cloud optical thickness ( $\tau_{\text{vis}}$ ) and the droplet effective radius estimates ( $r_e$ ). The effective radius is an intermediate product that is retrieved together with the cloud optical thickness from 0.6 and 1.6  $\mu\text{m}$  cloud radiances. The cloud liquid water path is estimated with the equation of Stephens (1978):

$$CLWP = \frac{2}{3} \cdot \tau_{\text{vis}} \cdot r_e \cdot \rho_l$$

Where  $\rho_l$  is the density of liquid water and  $r_e$  is the droplet effective radius of water particles.

The equation given above is currently applied for water and ice clouds. The water path estimates for ice clouds will be less reliable because the equation was originally defined for water clouds. KNMI and IFM in Kiel are currently working on an improved approach for the retrieval of ice cloud properties within the Visiting Scientist activity "Improved retrieval of ice cloud properties".

### 8.1 Validation method

The MSG and microwave radiometer cloud liquid water path retrievals were compared for Chilbolton (UK) for the observation periods of April 14<sup>th</sup> till April 30<sup>th</sup> and May 2004. Half hourly MSG (Meteosat-8) images were processed for an area over Central Europe including the CloudNET validation sites. The MSG cloud liquid water path was extracted for the satellite pixel that collocated best with the Chilbolton observation site (51.14°N, -1.44°W). The microwave radiometer liquid water path observations were averaged to 20 minutes means to obtain better correlations between ground and satellite derived liquid water path. Observations with rain were excluded from the validation dataset, because the microwave radiometer observations tend to become unrealistic for rain clouds. We did not use cloud radar and lidar observations to separate ice from water clouds. Note that the microwave radiometer is insensitive to ice clouds and will not measure any liquid water path for these clouds. However, the satellite retrieval is based on a different approach and may retrieve a liquid (or ice) water path for ice clouds.

### 8.2 Results

Figure 8.1 shows time series of MSG and microwave derived cloud liquid water path from 8:00-16:30 UTC for May 1<sup>st</sup>, 2004. This figure is a good example of the unique capability of MSG to obtain quantitative information on daily variations of cloud properties. As can be seen from the time series (left panel) and the scatter plot (right panel) there is good correlation between MSG

and microwave radiometer liquid water path ( $r=0.90$ ). On average the microwave liquid water path is higher than MSG liquid water path, as is indicated by the 0.63 gain of the regression fit. The half hourly variations of the differences between ground-based and satellite retrievals of liquid water path indicate that e.g. cloud conditions or viewing geometries affect the correlation between ground-based and satellite derived values.

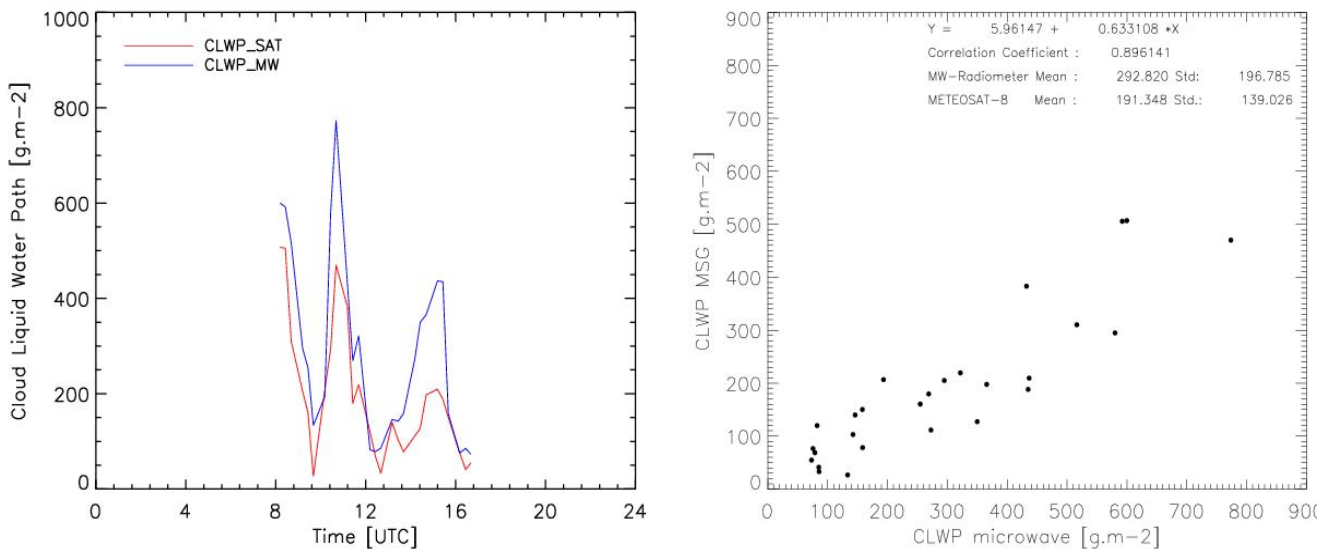


**Figure 8.1** Example of time series (left) and scatter plot (right) of MSG and microwave radiometer liquid water path for May 1<sup>st</sup> 2004 for Chilbolton, UK.

A more statistical approach is to compare frequency distributions of microwave radiometer and MSG cloud liquid water path. Figure 8.2 shows the frequency distributions of MSG and microwave radiometer cloud liquid water path. These distributions are presented for the observation period of April 14<sup>th</sup> till April 30<sup>th</sup> 2004 (upper panel) and May 1<sup>st</sup> till May 31<sup>st</sup> 2004 (lower panel). Although the frequency distributions of microwave and MSG liquid water path are not identical there are many similarities. The median values of MSG and microwave radiometer retrieved liquid water path are both low with values of  $\sim 13 \text{ gm}^{-2}$  and  $\sim 16 \text{ gm}^{-2}$  respectively. From the frequency distributions it can be seen that the microwave radiometer liquid water path is often higher than the MSG liquid water path.

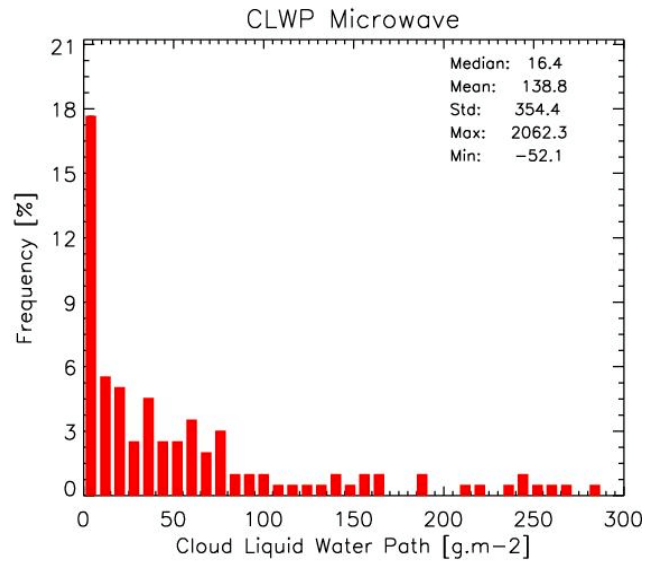
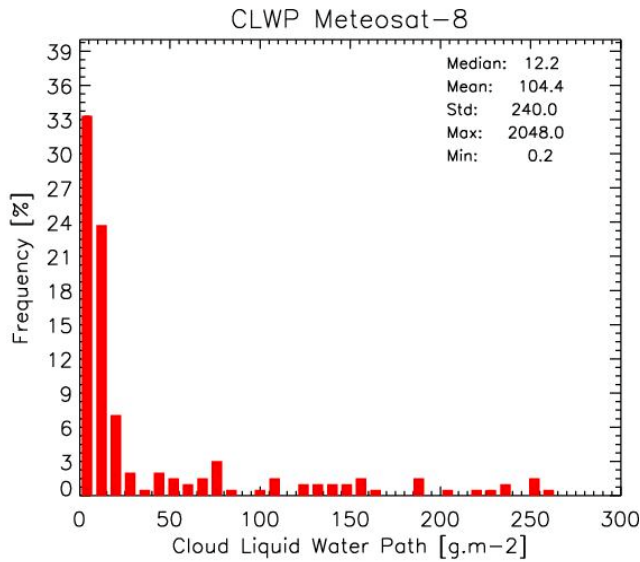
Figure 8.3 shows the frequency distributions of differences between microwave radiometer and MSG retrieved cloud liquid water path. These frequencies are normally distributed and have a strong peak for differences between 0 and  $-10 \text{ gm}^{-2}$ . For about 60% of the observations the differences range between  $-20$  and  $20 \text{ gm}^{-2}$ . Table 8.1 summarizes the results of the statistical comparison of microwave and MSG liquid water path.



**Scientific Report  
Initial Validation of CM-SAF  
Cloud Products using  
MSG/SEVIRI Data**

Doc. No:  
**SAF/CM/DWD/SMHI/KNMI/SR/CLOUDS/1**  
Issue: **1.0**  
Date: **23 March 2005**

14 – 30 April 2004



1- 31 May 2004

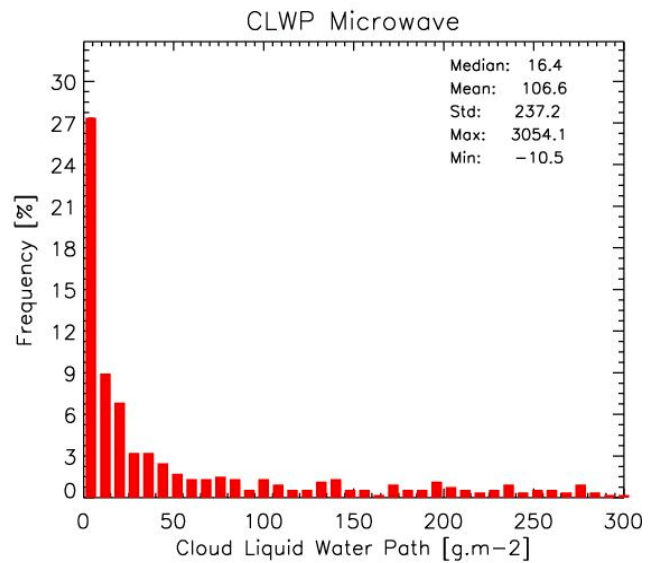
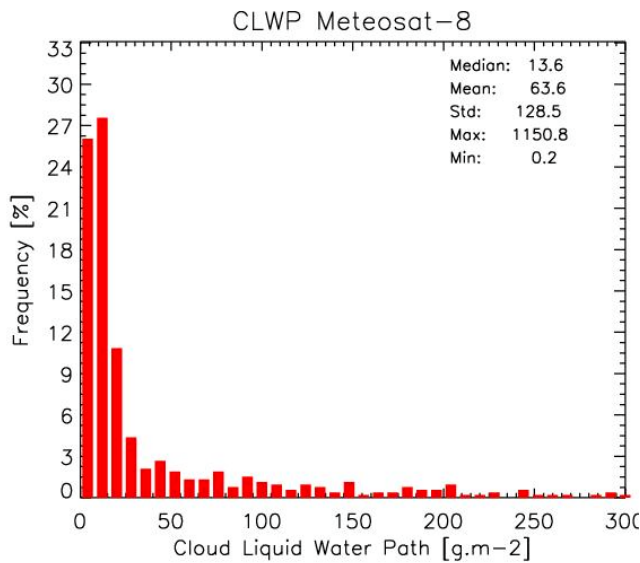


**Figure 8.2** Frequency distributions of MSG (METEOSAT-8) and microwave radiometer derived cloud liquid water path for Chilbolton, UK. The upper two distributions were made for the period of April 14<sup>th</sup> till April 30<sup>th</sup> 2004 and the lower two distributions for the period of May 2004.

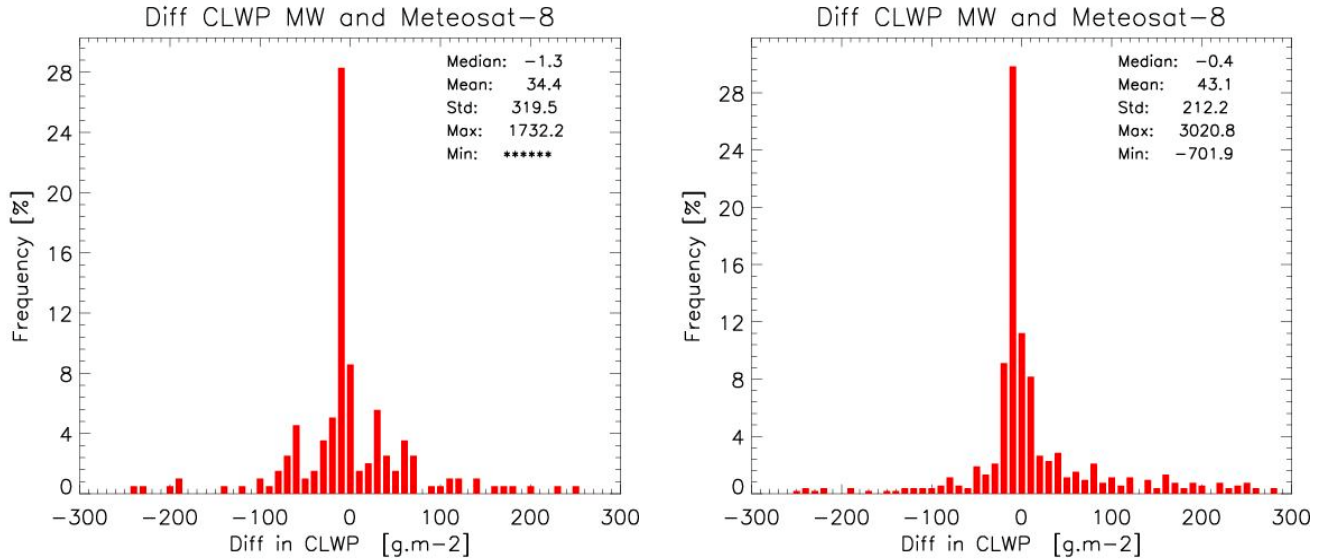


**Figure 8.3** Frequency distributions of differences between microwave and MSG (METEOSAT-8) derived cloud liquid water path for April 14<sup>th</sup> till April 30<sup>th</sup> (left panel) and May 2004 (right panel) for Chilbolton, UK.

**Table 8.1** Summary of the comparison of MSG (Meteosat-8) and Microwave derived Cloud Liquid Water Path

	Median CLWP MSG (g.m <sup>-2</sup> )	Median CLWP MW (g.m <sup>-2</sup> )	Mean difference MSG – MW (g.m <sup>-2</sup> )	Std. of difference MSG – MW (g.m <sup>-2</sup> )
14 – 30 April 2004	12.2	16.4	-34.4	319.5
01 – 31 May 2004	13.6	16.4	-43.1	212.2

### 8.3 Summary of CLWP validation results

Comparison of half-hourly MSG CLWP values with half-hourly results from the microwave radiometer shows that for about 60% of the observations, differences between microwave and MSG CLWP range between  $-20$  and  $+20$   $\text{g.m}^{-2}$ . However, microwave retrieved CLWP is often higher, as is indicated by the mean difference between microwave and MSG CLWP of 34 and 43  $\text{g.m}^{-2}$  for April and May 2004 respectively. The magnitude of the mean differences is strongly influenced by the CLWP values for very thick clouds that are significantly higher for microwave radiometer than for MSG. These clouds occur rarely and have little influence on the median of differences between microwave and MSG CLWP that are  $-1.3$   $\text{g.m}^{-2}$  for April and  $-0.4$   $\text{g.m}^{-2}$  for May. The differences may be explained by collocation errors and the sensitivity of the ground-based method to variations in cloud properties. In order to minimise collocation errors, comparison of daily averages of MSG and microwave radiometer retrieved CLWP values show a

	<b>Scientific Report</b> <b>Initial Validation of CM-SAF</b> <b>Cloud Products using</b> <b>MSG/SEVIRI Data</b>	Doc. No: <b>SAF/CM/DWD/SMHI/KNMI/SR/CLOUDS/1</b>
		Issue: <span style="float: right;"><b>1.0</b></span>
		Date: <span style="float: right;"><b>23 March 2005</b></span>

correlation about 0.7, which is significantly better than the correlation about 0.5 for the half-hourly observations.

## 9 SUMMARY AND CONCLUSIONS

The results of the SIVVRR V2 validation activities are summarised for all six CM-SAF cloud products in Table 9.1.

**Table 9.1** Validation results for the CM-SAF cloud products for the SIVVRR V2 review. Results are given for evaluation of individual (instantaneous), daily and monthly estimations (where applicable).

Product	Acronym	Accuracy according to SIVVRR V2 validation (quantity in parenthesis)		
		Instantaneous	Daily	Monthly
Fractional cloud cover	CFC	0.23 (Heidke skill score)	No estimation	All: -1 % Land: -1 % Ocean: 5-11 % (bias)
Cloud type	CTY	67 % correct (correct Low, Mid and High cloud categories)	Low: 0.8 Mid: 0.2-0.6 High: 0.7-0.8 (correlation) Low: 16-23 % Mid: 10-15 % High: 25 % (RMS)	Low: -1/+7 % Mid: -1/-2 % High: -2/-5 % (bias)
Cloud top temperature, height, and pressure	CTT, CTH, CTP	0.52-0.78 (correlation CTH) 1715-2441 (RMS CTH)	0.73-0.87 (correlation CTH) 1060-1506 (RMS CTH)	-150 m (bias CTH)
Cloud phase	CPH	Water: 0.91 Ice: 0.64 (Skill score)	No estimation	No estimation
Cloud optical thickness	COT	-19.7/-17.8 (bias) 0.43 (correlation)	0.85 (correlation)	No estimation
Cloud water path	CWP	-43.1/-34.4 gm <sup>-2</sup> (bias) 0.4/1.3 gm <sup>-2</sup> (median difference) 0.5 (correlation)	0.7 (correlation)	No estimation

	<b>Scientific Report</b> <b>Initial Validation of CM-SAF</b> <b>Cloud Products using</b> <b>MSG/SEVIRI Data</b>	Doc. No: <b>SAF/CM/DWD/SMHI/KNMI/SR/CLOUDS/1</b> Issue: <span style="float: right;"><b>1.0</b></span> Date: <span style="float: right;"><b>23 March 2005</b></span>
---	--	--

The following concluding remarks can be given with reference to the results shown in Table 9.1:

**CFC:**

This product appears to be the most well-tuned and reliable of the CM-SAF product, probably as a result of many years of product development and validation within the SAFNWC project. Monthly mean values agree very well with corresponding values based on surface observations. Some differences in performance are, however, seen over land and ocean surfaces. This feature is common to what has previously been found for the NOAA AVHRR product (see CM-SAF UMP, 2005). Furthermore, the fact that the Heidke skill score is fairly low for the instantaneous values shows that there is a considerable disagreement for individual cases and mostly in the intermediate cloud amount range (2-6 octas).

**CTY:**

This product is very difficult to objectively validate, partly because of a lack of a real firmly established definition of how to vertically separate various cloud types as a function of cloud top temperatures/pressures/heights. The approach used here is utilising assumptions made by the the particular product retrieval method and may not be fully representative of other ways of defining the various cloud types. With respect to this problem, results have to be used with caution.

Based on cloud radar retrievals of dominating cloud tops, results show a reasonable agreement with fairly low deviations concerning the monthly average values.

**CTT/CTH/CTP:**

The cloud top product have been validated by using cloud radar estimations of cloud top heights and results are only shown for the cloud top height product (CTH) assuming that results should be similar for the other two product representations.

Mainly as an effect of the many kind of problems of getting a representative way of comparing measurements and satellite observations, results show a considerable scatter when looking at individual cases. However, it is encouraging with respect to the climate monitoring task to find a very low bias for the monthly mean value (-150 m).

A serious remaining problem here is the treatment of the thinnest and highest cloud layers, especially in the cases when thin Cirrus layers are superposed over optically thick water clouds.

**CPH:**

The cloud phase product has been validated using a combined cloud radar/lidar method. Results show encouraging skills for water clouds but a significantly lower skill for ice clouds. This particular ice cloud problem is with a high probability explained by similar principles/conditions as the previously mentioned problem of a correct cloud top determination in case of thin Cirrus layers superposed over optically thick water clouds.

It should be mentioned that this is the very first CM-SAF evaluation of this product since it was introduced among the CM-SAF products just recently (during second half of 2004).

**COT:**

The optical thickness product has been validated using an empirical relationship between pyranometer broadband irradiance measurements and cloud optical depth. Results show a significant negative bias of results. It is, however, premature to conclude whether this is a truly significant feature or whether considerable deficiencies exist in the used calibration method.

	<b>Scientific Report</b> <b>Initial Validation of CM-SAF</b> <b>Cloud Products using</b> <b>MSG/SEVIRI Data</b>	Doc. No: <b>SAF/CM/DWD/SMHI/KNMI/SR/CLOUDS/1</b> Issue: <span style="float: right;"><b>1.0</b></span> Date: <span style="float: right;"><b>23 March 2005</b></span>
---	--	--

### **CWP:**

The cloud (liquid) water path product has been validated using microwave radiometer measurements. Just as for the COT product, results indicate a significant underestimation on the average. However, it is clear that there is a large influence on the average results from a few large measured CWP values since median difference values show no negative biases but instead a slightly positive value.

Finally, it should be mentioned that the conducted validation exercise has been performed slightly different depending on the actual product and the responsible partner/institute. For the next ORR V2 review, an attempt to further harmonise validation activities will be made and the task to estimate the quality of the climatological average products (daily, diurnal and monthly averages) will be given special attention.

## **10 REFERENCES**

- Barnard, J.C. and C.N. Long, 2004: A simple empirical equation to calculate cloud optical thickness using shortwave broadband measurements, *J. Appl. Meteor.*, **43**, 1057-1066.
- Baum, B.A., P.F. Soulen, K.I. Strabala, M.D. King, S.A. Ackerman, W.P. Menzel and P. Yang, 2000: Remote sensing of cloud properties using MODIS airborne simulator imagery during SUCCESS: 2. Cloud thermodynamic phase, *J. Geophys. Res.*, **105**, 11781-11792.
- CM-SAF UMP, 2005: User Manual of Products of the Climate Monitoring SAF; Version 1.5 (included in the SIVVRR V2 documentation).
- Deneke, 2002: Influence of clouds on the solar radiation budget, *KNMI Scientific Report, WR-2002-09*.
- Derrien, M. and H. LeGleau, 2003: SAFNWC/MSG SEVIRI cloud products, *Proc. 2003 EUMETSAT Meteorological Satellite Conference, Weimar, Germany, 29 Sep – 3 Oct. 2003*, EUM P 39, 191-198.
- Donovan, D.P., H. Bloemink, and A.C.A.P. van Lammeren, 1998: Analysis of ERM synergy by use of CLARA observations, *Final Report, ESA Contract No. 12953/98/NL/6D*.
- Dybbroe, A., Thoss, A. and Karlsson, K.-G., 2005: SAFNWC AVHRR cloud detection and analysis using dynamic thresholds and radiative transfer modelling – Part I: Algorithm description, *J. Appl. Meteor.*, **44**, 39-54.
- Dybbroe, A., Thoss, A. and Karlsson, K.-G., 2005: SAFNWC AVHRR cloud detection and analysis using dynamic thresholds and radiative transfer modelling – Part II: Validation, accepted by *J. Appl. Meteor.*, **44**, 55-71.
- Jolivet D., A.J. Feijt and P. Watts, 2000: Requirements for synergetic use of the ERM imager, *ESA Contract RFQ/3-9439/98/NL/GD*.

	<b>Scientific Report</b> <b>Initial Validation of CM-SAF</b> <b>Cloud Products using</b> <b>MSG/SEVIRI Data</b>	Doc. No: <b>SAF/CM/DWD/SMHI/KNMI/SR/CLOUDS/1</b> Issue: <span style="float: right;"><b>1.0</b></span> Date: <span style="float: right;"><b>23 March 2005</b></span>
---	--	--

- Hogan, R.J., A.J Illingworth, E.J. O'Connor and P.V. Poiares Baptista, 2003: Characteristics of mixed-phase clouds, part II: A climatology from ground-based lidar, *Quart. J. R. Met. Soc.*, **129**, 2117-2134.
- Nakajima T. and M.D. King, 1990: Determination of the optical thickness and effective particle radius of clouds from reflected solar radiation measurements, part 1: Theory, *J. Atm. Sci.*, **47**, 1878-1893.
- Nakajima T. Y. and T. Nakajima, 1995: Determination of cloud microphysical properties from NOAA AVHRR measurements for FIRE and ASTEX regions, *J. Atm. Sci.*, **52**, 4043 – 4059.
- Roebeling R.A., H. Hauschildt, D. Jolivet, E.A. van Meijgaard and A.J. Feijt, 2003: Retrieval and validation of METEOSAT-8 and AVHRR based cloud physical parameters in the CM-SAF. *Proceedings EUMETSAT Data Users Conference, 29 September – 3 October, 2003, Weimar, Germany.*
- SAFNWC SUM/1, 2004: Scientific User Manual for the PGE01-02-03 of the SAFNWC/MSG/SEVIRI
- SAFNWC SUM/2, 2004: Scientific User Manual for the AVHRR/AMSU cloud and precipitation products of the SAFNWC/PPS.
- Stephens G. L., G. W. Paltridge and C. M. R. Platt, 1978: Radiation profiles in extended water clouds. III. Observations. *J. Atm. Sci.*, **35**, 2133-2141.
- Trolez, M. A. Tetzlaff and K.-G. Karlsson, 2005: Validating the Cloud Top Height product using LIDAR data, CM-SAF Visiting Scientist report, *SMHI Reports Meteorology*, No. 118.